PHYSICAL REVIEW D **86,** 113003 (2012)

A supersymmetric $SU(5) \times T'$ unified model of flavor with large θ_{13}

Aurora Meroni,[1,*] S. T. Petcov,[1,2,†] and Martin Spinrath[1,‡]

[1]*SISSA/ISAS and INFN, Via Bonomea 265, I-34136 Trieste, Italy*

[2]*Kavli IPMU, University of Tokyo, 5-1-5 Kashiwanoha, Kashiwa 277-8583, Japan*

(Received 12 September 2012; published 3 December 2012)

We present a SUSY $SU(5) \times T'$ unified flavor model with type I seesaw mechanism of neutrino mass generation, which predicts the reactor neutrino angle to be $\theta_{13} \approx 0.14$ close to the recent results from the Daya Bay and RENO experiments. The model predicts also values of the solar and atmospheric neutrino mixing angles, which are compatible with the existing data. The T' breaking leads to tribimaximal mixing in the neutrino sector, which is perturbed by sizeable corrections from the charged lepton sector. The model exhibits geometrical CP violation, where all complex phases have their origin from the complex Clebsch-Gordan coefficients of T'. The values of the Dirac and Majorana CP violating phases are predicted. For the Dirac phase in the standard parametrization of the neutrino mixing matrix we get a value close to 90°: $\delta \cong \pi/2 - 0.45\theta^c \cong 84.3°$, θ^c being the Cabibbo angle. The neutrino mass spectrum can be with normal ordering (2 cases) or inverted ordering. In each case the values of the three light neutrino masses are predicted with relatively small uncertainties, which allows one to get also unambiguous predictions for the neutrinoless double beta decay effective Majorana mass.

DOI: 10.1103/PhysRevD.86.113003 PACS numbers: 14.60.Pq, 12.10.Dm, 12.15.Ff, 12.60.Jv

I. INTRODUCTION

Understanding the origin of the patterns of neutrino masses and mixing, emerging from the neutrino oscillation, ^{3}H β decay, etc. data is one of the most challenging problems in neutrino physics. It is part of the more general fundamental problem in particle physics of understanding the origins of flavor, i.e., of the patterns of the quark, charged lepton, and neutrino masses and of the quark and lepton mixing.

At present we have compelling evidence for the existence of mixing of three light massive neutrinos ν_i, $i = 1, 2, 3$, in the weak charged lepton current (see, e.g., Ref. [1]). The masses m_i of the three light neutrinos ν_i do not exceed approximately 1 eV, $m_i \lesssim 1$ eV, i.e., they are much smaller than the masses of the charged leptons and quarks. The three light neutrino mixing is described (to a good approximation) by the Pontecorvo, Maki, Nakagawa, Sakata (PMNS) 3×3 unitary mixing matrix, $U_{\rm PMNS}$. In the widely used standard parametrization [1], $U_{\rm PMNS}$ is expressed in terms of the solar, atmospheric, and reactor neutrino mixing angles θ_{12}, θ_{23}, and θ_{13}, respectively, one Dirac— δ, and two Majorana [2]— β_1 and β_2 CP violating phases:

$$U_{\rm PMNS} \equiv U = V(\theta_{12}, \theta_{23}, \theta_{13}, \delta)Q(\beta_1, \beta_2), \quad (1.1)$$

where

$$V = \begin{pmatrix} 1 & 0 & 0 \\ 0 & c_{23} & s_{23} \\ 0 & -s_{23} & c_{23} \end{pmatrix} \begin{pmatrix} c_{13} & 0 & s_{13}e^{-i\delta} \\ 0 & 1 & 0 \\ -s_{13}e^{i\delta} & 0 & c_{13} \end{pmatrix} \times \begin{pmatrix} c_{12} & s_{12} & 0 \\ -s_{12} & c_{12} & 0 \\ 0 & 0 & 1 \end{pmatrix}, \quad (1.2)$$

and we have used the standard notation $c_{ij} \equiv \cos\theta_{ij}$, $s_{ij} \equiv \sin\theta_{ij}$, and[1]

$$Q = {\rm Diag}(e^{-i\beta_1/2}, e^{-i\beta_2/2}, 1). \quad (1.3)$$

The neutrino oscillation data, accumulated over many years, allowed us to determine the parameters that drive the solar and atmospheric neutrino oscillations, $\Delta m^2_\odot \equiv \Delta m^2_{21}$, θ_{12} and $|\Delta m^2_A| \equiv |\Delta m^2_{31}| \cong |\Delta m^2_{32}|$, θ_{23}, with a rather high precision (see, e.g., Ref. [1]). Furthermore, there were spectacular developments in the last year in what concerns the angle θ_{13}. In June 2011 the T2K Collaboration reported [3] evidence at 2.5σ for a nonzero value of θ_{13}. Subsequently the MINOS [4] and Double Chooz [5] collaborations also reported evidence for $\theta_{13} \neq 0$, although with a smaller statistical significance. Global analysis of the neutrino oscillation data, including the data from the T2K and MINOS experiments, performed in Ref. [6], showed that actually $\sin\theta_{13} \neq 0$ at $\geq 3\sigma$. In March 2012 the first data of the Daya Bay reactor antineutrino experiment on θ_{13} were published [7]. The value of $\sin^2 2\theta_{13}$ was

*aurora.meroni@sissa.it

†Also at Institute of Nuclear Research and Nuclear Energy, Bulgarian Academy of Sciences, 1784 Sofia, Bulgaria.

‡spinrath@sissa.it

[1]This parametrization differs from the standard one. We use it for "technical" reasons related to the fitting code we will employ. Obviously, the standard one can be obtained as ${\rm Diag}(1, e^{i\alpha_{21}}, e^{i\alpha_{31}}) = e^{i\beta_1/2}Q$, with $\alpha_{21} = \beta_1 - \beta_2$ and $\alpha_{31} = \beta_1$.

measured with a rather high precision and was found to be different from 0 at 5.2σ:

$$\begin{aligned} \sin^2 2\theta_{13} &= 0.092 \pm 0.016 \pm 0.005, \\ 0.04 \leq \sin^2 2\theta_{13} &\leq 0.14, \quad 3\sigma, \end{aligned} \tag{1.4}$$

where we have given also the 3σ interval of allowed values of $\sin^2 2\theta_{13}$. Subsequently, the RENO experiment reported a 4.9σ evidence for a nonzero value of θ_{13} [8], compatible with the Day Bay result:

$$\sin^2 2\theta_{13} = 0.113 \pm 0.013 \pm 0.019. \tag{1.5}$$

The results on θ_{13} described above will have far reaching implications for the program of future research in neutrino physics (see, e.g., Ref. [9]).

A recent global analysis of the current neutrino oscillation data, in which the Daya Bay and RENO results on θ_{13} are also included, was published [10]. In Table I we show the best-fit values and the 99.73% C.L. allowed ranges of Δm^2_{21}, $\sin^2\theta_{12}$, $|\Delta m^2_{31(32)}|$, $\sin^2\theta_{23}$, and $\sin^2\theta_{13}$, found in Ref. [10].

Stimulated by the fact that all three angles in the PMNS matrix are determined with a relatively high precision, we report in the present article an attempt to construct a unified model of flavor, which describes correctly the quark and charged lepton masses, the mixing and CP violation in the quark sector, and the mixing in the lepton sector, including the relatively large value of the angle θ_{13}, and provides predictions for the light neutrino masses compatible with the existing relevant data and constraints. The unified model of flavor we are proposing is supersymmetric and is based on $SU(5)$ as a gauge group and T' as a discrete family symmetry. It includes three right-handed (RH) neutrino fields N_{lR}, $l = e, \mu, \tau$, which possess a Majorana mass term. The light neutrino masses are generated by the type I seesaw mechanism [12] and are naturally small.

TABLE I. The best-fit values and 3σ allowed ranges of the 3-neutrino oscillation parameters derived from a global fit of the current neutrino oscillation data, including the Daya Bay and RENO results (from Ref. [10]). These values are obtained using the "new" [11] reactor $\bar{\nu}_e$ fluxes. If two values are given the first one corresponds to normal hierarchy and the second one to inverted hierarchy.

Parameter	Best fit ($\pm 1\sigma$)	3σ
$\Delta m^2_{\odot}$ [10^{-5} eV^2]	7.62 ± 0.19	7.12–8.20
$\lvert\Delta m^2_A\rvert$ [10^{-3} eV^2]	$2.53^{+0.08}_{-0.10}$	2.26–2.77
	$-(2.40^{+0.10}_{-0.07})$	$-(2.15$–$2.68)$
$\sin^2\theta_{12}$	$0.320^{+0.015}_{-0.017}$	0.27–0.37
$\sin^2\theta_{23}$	$0.49^{+0.08}_{-0.02}$	0.39–0.64
	$0.53^{+0.05}_{-0.07}$	
$\sin^2\theta_{13}$	$0.026^{+0.003}_{-0.004}$	0.015–0.036
	$0.027^{+0.003}_{-0.004}$	0.016–0.037

The corresponding Majorana mass term of the left-handed flavor neutrino fields $\nu_{lL}(x)$, $l = e, \mu, \tau$ is diagonalized by a unitary matrix which, up to a diagonal phase matrix, is of the tribimaximal form [13]:

$$U_{\mathrm{TBM}} = \begin{pmatrix} \sqrt{2/3} & \sqrt{1/3} & 0 \\ -\sqrt{1/6} & \sqrt{1/3} & -\sqrt{1/2} \\ -\sqrt{1/6} & \sqrt{1/3} & \sqrt{1/2} \end{pmatrix}. \tag{1.6}$$

In order to account for the current data on the neutrino mixing, and more specifically, for the fact that $\theta_{13} \neq 0$, U_{TBM} has to be "corrected." The requisite correction is provided by the unitary matrix originating from the diagonalization of the charged lepton mass matrix M_e (for a general discussion of such corrections see, e.g., Refs. [14–16]). Since the model is based on the $SU(5)$ grand unified theory (GUT) symmetry, the charged lepton mass matrix M_e is related to the down-quark mass matrix M_d. As a consequence, in particular, of the connection between M_e and M_d, the smallest angle in the neutrino mixing matrix θ_{13} is related to the Cabibbo angle θ^c: $\sin^2\theta_{13} \cong C^2(\sin^2\theta^c)/2 \cong (\sin^2\theta^c)/2.5$, where $C \cong 0.9$ is a constant determined from the fit.

The down-quark mass matrix M_d, and the charged lepton mass matrix M_e, by construction are neither diagonal nor CP conserving. The matrix M_e is the only source of CP violation in the lepton sector. Actually, the CP violation predicted by the model in the quark and lepton sectors is entirely geometrical in origin. This aspect of the $SU(5) \times T'$ model we propose is a consequence, in particular, of one of the special properties of the group T',[2] namely, that its group theoretical Clebsch-Gordan coefficients are intrinsically complex [20]. The idea to use the complexity of the Clebsch-Gordan coefficients of T' to generate the requisite CP violation in the quark sector and a related CP violation in the lepton sector was pioneered in Ref. [21]. For the class of models where the CP violation is geometrical in origin, it is essential to provide a solution to the vacuum alignment problem for which all the flavon vacuum expectation values (vevs) are real. In this paper we present a solution for this problem for the models based on the $SU(5) \times T'$ symmetry.

Let us note finally that a model of flavor based on the symmetry group $SU(5) \times T'$ was proposed, to our knowledge, first in Ref. [22] and its properties were further elaborated in Refs. [21,23]. Although some generic features, like the connection between the reactor mixing angle θ_{13} and the Cabibbo angle θ^c, which are based on the underlying $SU(5)$ symmetry, are present both in the model constructed in Refs. [21,22] and in the model presented here; the detailed structure and the quantitative predictions of the two models are very different. The quark, charged

[2]There have been also T' models without a GUT embedding, e.g., Refs. [17–19].

lepton, RH neutrino mass matrices, and the matrix of the neutrino Yukawa couplings have different forms in the two models. This leads to considerable differences in the predictions for various observables. In the quark sector, for instance, the value of the Cabibbo-Kobayashi-Maskawa (CKM) phase we find is in much better agreement with experimental data. More importantly, in the model proposed in Refs. [21,22], the reactor mixing angle θ_{13} is predicted to have the value $\sin\theta_{13} \cong \sin\theta^c/(3\sqrt{2}) \cong 0.016$, which is ruled out by the current data on θ_{13}. In contrast, due to nonstandard $SU(5)$ Clebsch-Gordan relations between the down-type quark and the charged lepton Yukawa couplings [16,24], we get a realistic value for this angle. Moreover, in the model we propose, both neutrino mass spectra with normal and inverted ordering are possible, while the model developed in Refs. [21,22] admits only neutrino mass spectrum with normal ordering [23].

The paper is organized as follows. Section II is a brief overview of the considered model. In Sec. III we discuss the quark and charged lepton sector including a χ^2 fit to the experimental data. Section IV is completely devoted to the neutrino sector. There we describe in detail the predictions for the mixing parameters (including CP violating phases), the mass spectra, and observables such as the sum of the neutrino masses, the neutrinoless double beta $[(\beta\beta)_{0\nu}]$ decay effective Majorana mass, and the rephasing invariant related to the Dirac phase in the PMNS matrix, J_{CP}. We summarize and conclude in Sec. V. In the appendices we discuss the properties of the discrete group T', the messenger sector that generates the effective operators for the Yukawa couplings, and the superpotential, solving the flavon vacuum alignment problem.

II. MATTER, HIGGS FIELD, AND FLAVON FIELD CONTENT OF THE MODEL

In this section we describe the matter, the Higgs field, and the flavon content of our $SU(5) \times T'$ unified model of flavor. A rather large shaping symmetry, $Z_{12} \times Z_8^3 \times Z_6^2 \times Z_4$, is needed to solve the vacuum alignment issue and forbids unwanted terms and couplings in the superpotential (specifically in the renormalizable one as described in Appendix B, as well as in the effective one after integrating out heavy messenger fields). We further impose an additional $U(1)_R$ symmetry, the continuous generalization of the usual R parity. The messenger fields and auxiliary flavons used for the flavon superpotential are discussed in the appendices.

The model includes the three generations of matter fields in the usual $\bar{\mathbf{5}}$ and $\mathbf{10}$, representations of $SU(5)$, $\bar{F} = (d^c, L)_L$, and $T = (q, u^c, e^c)_L$ and three heavy right-handed Majorana neutrino fields N, singlets under $SU(5)$. The light active neutrino masses are generated through the type I seesaw mechanism [12]. Furthermore we introduce a number of copies of Higgs fields in the $\mathbf{5}$ and $\bar{\mathbf{5}}$ representation of $SU(5)$ that contain as linear combinations the two Higgs doublets of the MSSM. To get realistic mass ratios between down-type quarks and charged leptons [24] and to get a large reactor mixing angle [16], we have introduced Higgs fields in the adjoint representation of $SU(5)$ that are as well responsible for breaking the GUT group.

The matter and Higgs fields including their transformation properties under all imposed symmetries are summarized in Table II. Note that the right-handed neutrinos N and the five-dimensional matter representations are organized in T' triplets, while the tenplets are organized in a doublet and a singlet. On the one hand this will give us tribimaximal mixing (TBM) in the neutrino sector before considering corrections from the charged lepton sector and on the other hand the complex Clebsch-Gordan coefficients for the doublets will give us CP violation in the quark and in the lepton sector finally.

There are 13 flavons, which will give us the desired structure for the Yukawa couplings that will be discussed in the next section. First of all we have three triplets that will develop vevs into two different directions in flavor space,

$$\langle\phi\rangle = \begin{pmatrix} 0 \\ 0 \\ 1 \end{pmatrix} \phi_0, \qquad \langle\tilde{\phi}\rangle = \begin{pmatrix} 0 \\ 0 \\ 1 \end{pmatrix} \tilde{\phi}_0, \qquad \langle\xi\rangle = \begin{pmatrix} 1 \\ 1 \\ 1 \end{pmatrix} \xi_0. \tag{2.1}$$

TABLE II. Matter and Higgs field content of the model including quantum numbers.

	T_3	T_a	$\bar{F}$	N	$H_5^{(1)}$	$H_5^{(2)}$	$H_5^{(3)}$	$\bar{H}_5^{(1)}$	$\bar{H}_5^{(2)}$	$\bar{H}_5^{(3)}$	$\bar{H}_5''$	H_{24}''	$\tilde{H}_{24}''$
$SU(5)$	**10**	**10**	$\bar{\mathbf{5}}$	**1**	**5**	**5**	**5**	$\bar{\mathbf{5}}$	$\bar{\mathbf{5}}$	$\bar{\mathbf{5}}$	$\bar{\mathbf{5}}$	**24**	**24**
T'	**1**	**2**	**3**	**3**	**1**	**1**	**1**	**1**	**1**	**1**	$\mathbf{1}''$	$\mathbf{1}''$	$\mathbf{1}''$
$U(1)_R$	1	1	1	1	0	0	0	0	0	0	0	0	0
Z_{12}^u	2	11	1	9	8	8	2	9	3	6	3	0	3
Z_8^d	4	0	2	6	0	4	0	1	4	7	7	4	2
Z_8^ν	7	6	2	0	2	6	4	1	1	5	7	4	0
Z_8	0	5	2	2	0	0	6	0	0	6	6	4	2
Z_6	5	0	1	0	2	5	2	2	0	2	2	0	0
Z_6'	2	3	1	0	2	5	2	5	0	2	2	0	0
Z_4	3	3	0	0	2	0	2	0	1	1	0	0	1

TABLE III. Flavon fields coupling to the matter sector including their quantum numbers. In fact, ζ' does not couple directly to the matter fields, but it behaves similarly like the other flavons and not like the auxiliary flavons ϵ that will be introduced in Appendix C.

	$\tilde{\phi}$	$\tilde{\psi}''$	$\tilde{\psi}'$	$\tilde{\zeta}''$	$\tilde{\zeta}'$	ϕ	ψ''	ψ'	ζ''	ζ'	ξ	ρ	$\tilde{\rho}$
$SU(5)$	$\mathbf{1}$	$\mathbf{1}$	$\mathbf{1}$	$\mathbf{1}$	$\mathbf{1}$	$\mathbf{1}$	$\mathbf{1}$	$\mathbf{1}$	$\mathbf{1}$	$\mathbf{1}$	$\mathbf{1}$	$\mathbf{1}$	$\mathbf{1}$
T'	$\mathbf{3}$	$\mathbf{2}''$	$\mathbf{2}'$	$\mathbf{1}''$	$\mathbf{1}'$	$\mathbf{3}$	$\mathbf{2}''$	$\mathbf{2}'$	$\mathbf{1}''$	$\mathbf{1}'$	$\mathbf{3}$	$\mathbf{1}$	$\mathbf{1}$
$U(1)_R$	0	0	0	0	0	0	0	0	0	0	0	0	0
Z_{12}^u	0	3	9	0	0	6	3	9	6	0	6	6	6
Z_8^d	0	0	0	0	0	2	1	7	6	4	4	4	4
Z_8^ν	4	1	7	0	0	2	7	1	6	4	0	0	0
Z_8	4	7	5	4	0	2	5	3	6	4	4	4	4
Z_6	4	4	2	4	2	0	3	3	0	0	0	0	0
Z_6'	4	4	2	4	2	3	0	0	0	0	0	0	0
Z_4	0	2	2	0	0	0	3	1	2	0	0	0	0

The first two flavons will be relevant for the quark and the charged lepton sector and the third one couples only to the neutrino sector.

Then we have introduced four complex T' doublets. Notice that these spinorial representations of the T' group are essential since, having complex Clebsch-Gordan coefficients (see Appendix A), they are responsible of the CP violation in both quark and charged lepton sectors. We assume that CP is conserved on the fundamental level (all couplings are real) and all flavon vevs are real. In Appendix C we give a superpotential that has the desired flavon vev directions as a solution and also fixes the phases of the vevs up to a few discrete choices. For the doublets we find the vev alignments

$$\begin{aligned} \langle\psi'\rangle &= \begin{pmatrix}1\\0\end{pmatrix}\psi'_0, \qquad \langle\psi''\rangle = \begin{pmatrix}0\\1\end{pmatrix}\psi''_0, \\ \langle\tilde{\psi}'\rangle &= \begin{pmatrix}1\\0\end{pmatrix}\tilde{\psi}'_0, \qquad \langle\tilde{\psi}''\rangle = \begin{pmatrix}0\\1\end{pmatrix}\tilde{\psi}''_0. \end{aligned} \tag{2.2}$$

Furthermore we have introduced six flavons in one-dimensional representations of T' that receive all nonvanishing (and real) vevs

$$\begin{aligned} &\langle\zeta'\rangle = \zeta'_0, \qquad \langle\zeta''\rangle = \zeta''_0, \qquad \langle\tilde{\zeta}'\rangle = \tilde{\zeta}'_0, \\ &\langle\tilde{\zeta}''\rangle = \tilde{\zeta}''_0, \qquad \langle\rho\rangle = \rho_0, \qquad \langle\tilde{\rho}\rangle = \tilde{\rho}_0. \end{aligned} \tag{2.3}$$

All flavons including their quantum numbers are summarized in Table III. As we will see soon the flavon field ζ' does not directly couple to the matter sector. Nevertheless, we mention it here because it behaves differently than the auxiliary ϵ flavons which we have introduced to get the desired alignment and make all vevs real, see Appendix C.

III. THE QUARK AND CHARGED LEPTON SECTOR

In this section we describe the superpotential of the quark and charged lepton content of the chiral superfields of the model under study. We will consider the three generations of matter fields in the usual $\bar{\mathbf{5}}$ and $\mathbf{10}$, five- and ten-dimensional, representations of $SU(5)$, $\bar{F} = (d^c, L)_L$, and $T = (q, u^c, e^c)_L$. The elements of the Yukawa coupling matrices are generated dynamically through a number of effective operators whose structure is tightly related to the matter fields assignment under the T' discrete symmetry. Indeed the Yukawa coupling matrices can be written only after the breaking of the T' discrete symmetry. As will be clear soon, in this description CP violation in the quark and charged lepton sector is entirely due to geometrical origin, specifically from the use of the spinorial representation of the T' group. Finally, in this section we will present a χ^2 fit analysis that has been performed by us to get the low-energy masses and mixing parameters in the quark and charged lepton sector. We show as well that the simple CKM phase sum rule from Ref. [25] can be applied here.

A. Effective operators and Yukawa matrices

Before we come to the effective operators that will give us the Yukawa couplings, we first fix the conventions used for the Yukawa matrices. Throughout this paper we will use the right-left convention, i.e.,

$$-\mathcal{L} = Y_{ij}\bar{f}^i_R f^j_L H + \text{H.c.} \tag{3.1}$$

or in other words we have to diagonalize the combination $Y^\dagger Y$. Keep in mind also that $\bar{F} = (d^c, L)_L$ and $T = (q, u^c, e^c)_L$.

We restrict ourselves to effective operators up to mass dimension seven. These operators generate Yukawa couplings of the order of 10^{-5} or smaller (see our fit results in Table V). Higher dimensional operators hence can be expected to give only negligible corrections.

After integrating out the heavy messenger fields, see Appendix B, we obtain the effective operators

$$\begin{aligned} \mathcal{W}_{Y_u} = {}& y_{33}^{(u)} H_5^{(1)} T_3 T_3 + \frac{y_{23}^{(u)}}{\Lambda_u^2}(T_a\tilde{\phi})_{2'} H_5^{(2)}(T_3\tilde{\psi}'')_{2''} \\ &+ \frac{y_{22}^{(u)}}{\Lambda_u^3}(T_a\tilde{\psi}'')_3 (H_5^{(1)}\tilde{\zeta}')_{1'}(T_a\tilde{\psi}'')_3 \\ &+ \frac{y_{21}^{(u)}}{\Lambda_u^4}(T_a\tilde{\phi})_{2'}(H_5^{(1)}\tilde{\zeta}')_{1'}(\tilde{\psi}'(T_a\tilde{\psi}')_3)_{2'} \\ &+ \frac{y_{11}^{(u)}}{\Lambda_u^4}((T_a\tilde{\phi})_2\tilde{\zeta}'')_{2''} H_5^{(3)}(\tilde{\zeta}''(T_a\tilde{\phi})_{2''})_{2'}, \end{aligned} \tag{3.2}$$

which give the up-type quark Yukawa matrices after the flavons developed their vevs. Here Λ_u stands for the messenger scale suppressing the nonrenormalizable operators in the up sector and in the down sector we will introduce Λ_d correspondingly. We have also given the T' contractions as indices on the round brackets. Note that in general there are many different contractions possible [for T' and to a less degree for $SU(5)$], which give different results. Nevertheless, we have specified in Appendix B the fields mediating the nonrenormalizable operators that transform in a specific way under T' such that we pick up only the contractions that we want.

Multiplying the T' and $SU(5)$ indices out, we obtain for the up-type quark Yukawa matrix at the GUT scale (which is roughly equal to the scale of T' breaking)

$$Y_u = \begin{pmatrix} \bar{\omega} a_u & \mathrm{i} b_u & 0 \\ \mathrm{i} b_u & c_u & \omega d_u \\ 0 & \omega d_u & e_u \end{pmatrix}, \tag{3.3}$$

where $\omega = (1 + \mathrm{i})/\sqrt{2}$ and $\bar{\omega} = (1 - \mathrm{i})/\sqrt{2}$. The parameters a_u, b_u, c_u, d_u, and e_u are (real) functions of the underlying parameters. Note at this point that the phases of the flavon vevs have to be fixed. Otherwise the coefficients in the Yukawa matrix are complex parameters and we would not be able to make definite predictions anymore.

For the down-type quarks and charged leptons [remember that those two sectors are closely related in $SU(5)$], we find for the superpotential

$$\begin{aligned} \mathcal{W}_{Y_{d,\ell}} = & \frac{y_{33}^{(d)}}{\Lambda_d^2}((\bar{H}_5^{(2)}\bar{F})_3\phi)_{1'}(H_{24}''T_3)_{1''} \\ & + \frac{y_{22}^{(d)}}{\Lambda_d^3}((\phi T_a)_{2'}H_{24}'')_2(\psi'(\bar{H}_5^{(1)}\bar{F})_3)_2 \\ & + \frac{y_{12}^{(d)}}{\Lambda_d^4}(((T_a\tilde{H}_{24}'')_{2''}(\bar{F}\psi')_{2''})_3\psi')_{2''}(\bar{H}_5^{(3)}\psi')_{2'} \\ & + \frac{y_{21}^{(d)}}{\Lambda_d^4}((\bar{F}\psi')_{2''}(\zeta''\bar{H}_5^{(1)})_{1''}\zeta'')_2(T_a\phi)_2 \\ & + \frac{y_{11}^{(d)}}{\Lambda_d^4}((\bar{F}\psi'')_{2'}(H_{24}''\psi'')_{2'}\bar{H}_5'')_{1'}(T_a\psi'')_{1''}, \end{aligned} \tag{3.4}$$

where we have again specified the T' contractions. From this superpotential and considering the correct $SU(5)$ contractions, which we could not display here for the sake of readability, we get the down-type quark and charged lepton Yukawa matrices

$$Y_d = \begin{pmatrix} \omega a_d & \mathrm{i} b_d' & 0 \\ \bar{\omega} b_d & c_d & 0 \\ 0 & 0 & d_d \end{pmatrix} \quad \text{and}$$

$$Y_e = \begin{pmatrix} -\frac{3}{2}\omega a_d & \bar{\omega} b_d & 0 \\ 6\mathrm{i} b_d' & 6 c_d & 0 \\ 0 & 0 & -\frac{3}{2} d_d \end{pmatrix}, \tag{3.5}$$

where a_d, b_d, b_d', c_d, and d_d are (real) functions of the underlying parameters.

Note that the prediction from the minimal $SU(5)$ model $Y_d = Y_e^T$ is broken. Indeed it has to be broken to get realistic fermion masses. For the second generation this was known for a long time [28]. In some recent work [24] some new relations to fix this issue were proposed. From those we will use here $y_\tau/y_b = -3/2$ and $y_\mu/y_s \approx 6$ where y_τ, y_μ, y_b, and y_s stand for the eigenvalues of the Yukawa matrices associated with the masses of the τ, the μ, the b, and the s quark, respectively. Furthermore, it was shown in Ref. [16] (see also Ref. [29]) that those new $SU(5)$ Clebsch-Gordan coefficients might also give a large reactor neutrino mixing angle θ_{13}. For the current paper we have chosen one of the possible combinations given in Ref. [16] but we remark that in principle other combinations also are still possible that might be realized in another unified flavor model with a similar good fit to the fermion masses and mixing angles.

B. Fit results and the CKM phase sum rule

In the last section we discussed the structure of the Yukawa matrices in the quark and the charged lepton sector. These matrices have five free parameters, which in principle can be fitted to the low-energy mass and mixing parameters using the renormalization group. But in doing so one has to take into account SUSY threshold corrections [30] that modify the masses and mixing angles significantly. For example without including them, the GUT scale Yukawa coupling ratio, y_τ/y_b, would be roughly 1.3, which is not close to the usual GUT prediction of 1. There is a large amount of literature on how to use SUSY threshold corrections to get $b - \tau$ Yukawa unification; for recent papers see, for instance, Refs. [24,31,32]. From these studies it is known that in order to get $b - \tau$ Yukawa unification, it is necessary to either consider a negative μ term or to have a very high, $\mathcal{O}(10\ \text{TeV})$, SUSY scale. Nevertheless, we will not use unification but instead we use the recently proposed GUT scale relation $y_\tau/y_b = 3/2$ induced by the vev of an adjoint of $SU(5)$ [24], which is viable in a large region of the parameter space even in constrained MSSM scenarios.

Because of the importance of the threshold corrections for our fit, we briefly revise the most important formulas that also define our parametrization. In Ref. [33] the approximate matching conditions at the SUSY scale, M_{SUSY},

$$y_{e,\mu,\tau}^{\text{SM}} = (1 + \epsilon_l \tan\beta) y_{e,\mu,\tau}^{\text{MSSM}} \cos\beta, \tag{3.6}$$

$$y_{d,s}^{\text{SM}} = (1 + \epsilon_q \tan\beta) y_{d,s}^{\text{MSSM}} \cos\beta, \tag{3.7}$$

$$y_b^{\text{SM}} = (1 + (\epsilon_q + \epsilon_A)\tan\beta) y_b^{\text{MSSM}} \cos\beta, \tag{3.8}$$

for the Yukawa couplings and

$$\theta_{i3}^{\text{SM}} = \frac{1 + \epsilon_q \tan\beta}{1 + (\epsilon_q + \epsilon_A)\tan\beta} \theta_{i3}^{\text{MSSM}}, \tag{3.9}$$

$$\theta_{12}^{\text{SM}} = \theta_{12}^{\text{MSSM}}, \tag{3.10}$$

$$\delta^{\mathrm{SM}}_{\mathrm{CKM}} = \delta^{\mathrm{MSSM}}_{\mathrm{CKM}}, \tag{3.11}$$

for the quark mixing parameters were given, where the SUSY threshold corrections are parametrized in terms of the three parameters ϵ_l, ϵ_q, and ϵ_A. We will adopt this parametrization neglecting ϵ_l, which is usually one order smaller than ϵ_q [31]. Furthermore, we want to assume that SUSY is broken similar to the constrained MSSM scenario with a positive μ parameter and hence we adopt the recently proposed GUT relation $y_\tau/y_b = 3/2$ for the third generation, as mentioned earlier. For the second generation we use $y_\mu/y_s \approx 6$ [24].

We have fixed the SUSY scale to 750 GeV, the GUT scale to 2×10^{16} GeV, and $\tan\beta$ to 35. Therefore, we have to fit the ten parameters in the Yukawa matrices and the two parameters from the SUSY threshold corrections to the thirteen low-energy observables in the quark and the charged lepton sector (nine masses, three mixing angles, and one phase), so that we have one prediction (degree of freedom).

The renormalization group equation (RGE) running and diagonalisation of the matrices was done using the REAP package [34]. Performing a χ^2 fit we have found as minimum the results listed in Table IV for the parameters, and in Table V and in Fig. 1 we have presented the results of the fit for the low-energy observables compared to the experimental results. Note that we have assumed an uncertainty of 3% on the Yukawa couplings for the charged leptons. Their experimental uncertainty is much smaller, so that their theoretical uncertainty (accuracy of RGEs, neglecting SUSY threshold corrections for the leptons, NLO effects, etc). is much bigger, which we estimate to be 3%.

We find good agreement between our model and experimental data with a minimal χ^2 per degree of freedom of 2.76. In fact, this agreement is not accidental. We have chosen the $SU(5)$ coefficients such that we expect good agreement and we have also enough free parameters to fix the mixing angles. In other words, one could determine the eigenvalues and mixing angles from the data and then the CKM phase would be a prediction. But as we will demonstrate now, the choice for our phases in the Yukawa matrices was done in such a way that we can expect a good prediction for the CKM phase as well.

We will show in the following that the sum rule given in Ref. [25] can be used here. To apply the sum rule we have to find approximate expressions for the complex mixing angles (see Ref. [25]). For the rest of the subsection we will use the the notation of Ref. [25], which we just briefly

TABLE IV. Values of the effective parameters of the quark and charged lepton Yukawa matrices for $\tan\beta = 35$ and $M_{\mathrm{SUSY}} = 750$ GeV. The two parameters ϵ_q and ϵ_A parametrize the SUSY threshold corrections. The numerical values are determined from a χ^2 fit to experimental data with a lowest χ^2 per degree of freedom of 2.76.

Parameter	Value
a_u	5.81×10^{-6}
b_u	-9.96×10^{-5}
c_u	-8.55×10^{-4}
d_u	1.99×10^{-2}
e_u	0.525
a_d	-2.82×10^{-5}
b_d	-5.73×10^{-4}
b'_d	-5.09×10^{-4}
c_d	2.50×10^{-3}
d_d	1.82×10^{-1}
$\epsilon_q \tan\beta$	0.1788
$\epsilon_A \tan\beta$	-0.0001

TABLE V. Fit results for the quark Yukawa couplings and mixing and the charged lepton Yukawa couplings at low energy compared to experimental data. The values for the Yukawa couplings are extracted from Ref. [26], the ratio y_s/y_d is taken from Ref. [27], and the CKM parameters from Ref. [1]. Note that the experimental uncertainty on the charged lepton Yukawa couplings are negligibly small, and we have assumed a relative uncertainty of 3% for them. The χ^2 per degree of freedom is 2.76. A pictorial representation of the agreement between our fit and experiment can be found as well in Fig. 1.

Quantity [at $m_t(m_t)$]	Experiment	Model	Deviation
y_τ in 10^{-2}	1.00	0.99	-0.388
y_μ in 10^{-4}	5.89	5.90	0.044
y_e in 10^{-6}	2.79	2.79	-0.003
y_b in 10^{-2}	1.58 ± 0.05	1.57	-0.157
y_s in 10^{-4}	2.99 ± 0.86	2.57	-0.484
y_s/y_d	18.9 ± 0.8	18.9	-0.012
y_t	0.936 ± 0.016	0.936	0.0001
y_c in 10^{-3}	3.39 ± 0.46	2.79	-1.317
y_u in 10^{-6}	$7.01^{+2.76}_{-2.30}$	7.01	-0.0003
$\theta^{\mathrm{CKM}}_{12}$	$0.2257^{+0.0009}_{-0.0010}$	0.2257	-0.0107
$\theta^{\mathrm{CKM}}_{23}$	$0.0415^{+0.0011}_{-0.0012}$	0.0416	0.1268
$\theta^{\mathrm{CKM}}_{13}$	0.0036 ± 0.0002	0.0036	0.2043
δ_{CKM}	$1.2023^{+0.0786}_{-0.0431}$	1.2610	0.7465

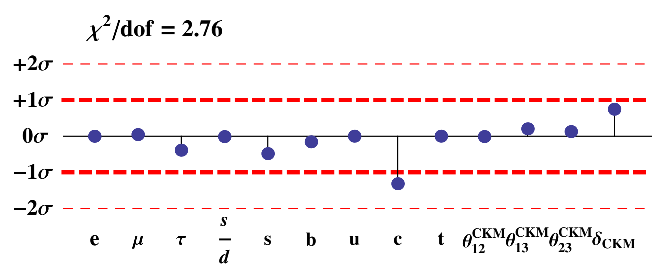

FIG. 1 (color online). Pictorial representation of the deviation of our fit from low-energy experimental data for the charged lepton Yukawa couplings and quark Yukawa couplings and mixing parameters. The deviations of the charged lepton masses are given in 3% while all other deviations are given in units of standard deviations σ.

summarize here for convenience. The CKM matrix $U_{\rm CKM}$ can be written as

$$U_{\rm CKM} = U_{u_L}U_{d_L}^\dagger = (U_{23}^{u_L}U_{13}^{u_L}U_{12}^{u_L})^\dagger U_{23}^{d_L}U_{13}^{d_L}U_{12}^{d_L}, \qquad (3.12)$$

where the matrices U_{u_L} and U_{d_L} diagonalize the up- and down-type quark mass matrices and the unitary matrix

$$U_{12} = \begin{pmatrix} \cos\theta_{12} & \sin\theta_{12}e^{-i\delta_{12}} & 0 \\ -\sin\theta_{12}e^{i\delta_{12}} & \cos\theta_{12} & 0 \\ 0 & 0 & 1 \end{pmatrix}. \qquad (3.13)$$

The matrices U_{13} and U_{23} are given by analogous expressions.

We find at leading order for the respective mixing angles and phases

$$\theta_{12}^d e^{-i\delta_{12}^d} = \left|\frac{b_d}{c_d}\right| e^{-i\frac{7\pi}{4}}, \qquad \theta_{13}^d = \theta_{23}^d = 0, \qquad (3.14)$$

$$\theta_{12}^u e^{-i\delta_{12}^u} \approx \left|\frac{b_u}{\sqrt{2}c_u}\right| e^{-i\frac{5\pi}{4}}, \qquad \theta_{23}^u e^{-i\delta_{23}^u} = \left|\frac{d_u}{e_u}\right| e^{-i\frac{5\pi}{4}},$$
$$\theta_{13}^u e^{-i\delta_{13}^u} = \left|\frac{b_u d_u}{e_u^2}\right| e^{-i\frac{\pi}{4}}, \qquad (3.15)$$

where we have used for θ_{12}^u that $d_u^2 \approx -1/2c_u$ and $e_u \approx 0.5$ from our fit. So we see that δ_{12}^u is not simply $\pi/2$ as one would expect from a quick first inspection. Note also that the phase sum rule was derived for $\theta_{13}^u = \theta_{13}^d = 0$, which is not exactly true in our case for θ_{13}^u. But in fact it is sufficient that $\theta_{13}^u \ll \theta_{12}^u\theta_{23}$, which is fulfilled here.

The angle α in the CKM unitarity triangle is experimentally measured to be $\alpha = (90.7^{+4.5}_{-2.9})^\circ$ [35] for which the sum rule

$$\alpha \approx \delta_{12}^d - \delta_{12}^u \qquad (3.16)$$

was given in Ref. [25]. Plugging in our approximate analytical expressions for $\delta_{12}^{d/u}$, Eqs. (3.14) and (3.15), we find that $\alpha \approx \pi/2$, and our model is in good agreement with experimental data as we have also seen it before from our numerical fit.

IV. NEUTRINO SECTOR

The model includes three heavy right-handed Majorana neutrino fields N that are singlets under $SU(5)$ and a triplet under T'. Through the type I seesaw mechanism [12], we generate light neutrino masses. The neutrino sector is described by the following terms in the superpotential:

$$\mathcal{W}_\nu = \lambda_1 NN\xi + NN(\lambda_2\rho + \lambda_3\tilde{\rho}) + \frac{y_\nu}{\Lambda}(N\bar{F})_1(H_5^{(2)}\rho)_1$$
$$+ \frac{\tilde{y}_\nu}{\Lambda}(N\bar{F})_1(H_5^{(2)}\tilde{\rho})_1, \qquad (4.1)$$

where we have given the T' contractions as indices at the brackets for nonrenormalizable terms and from now on Λ labels a generic messenger scale. Note that the contraction of three triplets in general is not unique; see also Table VII, because the product of two triplets contains a symmetric and an antisymmetric triplet. But since we multiply here two N's with each other only, the symmetric combination gives a nonvanishing contribution. In the following we will discuss the phenomenological implications of this superpotential (including corrections from the charged lepton sector).

A. The neutrino mass spectrum

From Eq. (4.1) we obtain for the mass matrix for the right-handed neutrinos and the Dirac neutrino mass matrix

$$M_R = \begin{pmatrix} 2Z+X & -Z & -Z \\ -Z & 2Z & -Z+X \\ -Z & -Z+X & 2Z \end{pmatrix},$$
$$M_D = \begin{pmatrix} 1 & 0 & 0 \\ 0 & 0 & 1 \\ 0 & 1 & 0 \end{pmatrix}\frac{\rho'}{\Lambda}, \qquad (4.2)$$

where X, Z, and ρ' are real parameters depending on the couplings and the vevs in Eq. (4.1). The right-handed neutrino mass matrix M_R is diagonalized by the TBM matrix [13]

$$U_{\rm TBM} = \begin{pmatrix} \sqrt{2/3} & \sqrt{1/3} & 0 \\ -\sqrt{1/6} & \sqrt{1/3} & -\sqrt{1/2} \\ -\sqrt{1/6} & \sqrt{1/3} & \sqrt{1/2} \end{pmatrix}, \qquad (4.3)$$

such that the heavy RH neutrino masses read

$$U_{\rm TBM}^T M_R U_{\rm TBM} = D_N = {\rm Diag}(3Z+X, X, 3Z-X)$$
$$= {\rm Diag}(M_1e^{i\phi_1}, M_2e^{i\phi_2}, M_3e^{i\phi_3}),$$
$$M_{1,2,3} > 0, \qquad (4.4)$$

where

$$M_1 = |X+3Z| \equiv |X||1+\alpha e^{i\phi}|, \qquad \phi_1 = \arg(X+3Z), \qquad (4.5)$$

$$M_2 = |X|, \qquad \phi_2 = \arg(X), \qquad (4.6)$$

$$M_3 = |X-3Z| \equiv |X||1-\alpha e^{i\phi}|, \qquad \phi_3 = \arg(3Z-X). \qquad (4.7)$$

Here $\alpha \equiv |3Z/X| > 0$ and $\phi \equiv \arg(Z) - \arg(X)$. Since X and Z are real parameters, the phases ϕ_1, ϕ_2, ϕ_3, and ϕ take values 0 or π. A light neutrino Majorana mass term is generated after electroweak symmetry breaking via the type I seesaw mechanism:

$$M_\nu = -M_D^T M_R^{-1} M_D = U_\nu^* {\rm Diag}(m_1, m_2, m_3)U_\nu^\dagger, \qquad (4.8)$$

where

$$U_\nu = \mathrm{i}U_{\mathrm{TBM}}\mathrm{Diag}(e^{\mathrm{i}\phi_1/2}, e^{\mathrm{i}\phi_2/2}, e^{\mathrm{i}\phi_3/2}) \equiv \mathrm{i}U_{\mathrm{TBM}}\tilde{Q}, \quad \tilde{Q} \equiv \mathrm{Diag}(e^{\mathrm{i}\phi_1/2}, e^{\mathrm{i}\phi_2/2}, e^{\mathrm{i}\phi_3/2}), \tag{4.9}$$

and $m_{1,2,3} > 0$ are the light neutrino masses,

$$m_i = \left(\frac{\rho'}{\Lambda}\right)^2 \frac{1}{M_i}, \qquad i = 1, 2, 3. \tag{4.10}$$

The phase factor i in Eq. (4.9) corresponds to an unphysical phase and we will drop it in what follows. Note also that one of the phases ϕ_k, say ϕ_1, is physically irrelevant since it can be considered a common phase of the neutrino mixing matrix. In the following we always set $\phi_1 = 0$. This corresponds to the choice $(X + 3Z) > 0$.

The type of the neutrino mass spectrum in the model is determined[3] by the value of the phase ϕ. Indeed, as it is not difficult to show, we have

$$\Delta m^2_{31} \equiv \Delta m^2_A = \frac{1}{|X|^2}\left(\frac{\rho'}{\Lambda}\right)^4 \frac{4\alpha\cos\phi}{|1+\alpha e^{\mathrm{i}\phi}|^2|1-\alpha e^{\mathrm{i}\phi}|^2}. \tag{4.11}$$

Thus, for $\cos\phi = +1$, we get $\Delta m^2_{31} > 0$, i.e., a neutrino mass spectrum with normal ordering (NO), while for $\cos\phi = -1$ one has $\Delta m^2_{31} < 0$, i.e., neutrino mass spectrum with inverted ordering (IO). We have also

$$\Delta m^2_{21} \equiv \Delta m^2_\odot = \frac{1}{|X|^2}\left(\frac{\rho'}{\Lambda}\right)^4 \frac{\alpha(\alpha + 2\cos\phi)}{|1+\alpha e^{\mathrm{i}\phi}|^2}. \tag{4.12}$$

For a given type of neutrino mass spectrum, i.e., for a fixed $\phi = 0$ or π, a constraint on the parameter α can be obtained from the requirement that $\Delta m^2_{21} > 0$ and from the data on the ratio

$$r = \frac{\Delta m^2_\odot}{|\Delta m^2_A|} = \frac{1}{4}(\alpha + 2\cos\phi)(1 - 2\alpha\cos\phi + \alpha^2) = 0.032 \pm 0.006. \tag{4.13}$$

Using the values of α thus found and the value of, e.g., Δm^2_{21}, one can get (for a given type of the spectrum) the value of the factor in Eq. (4.12), $|X|^{-2}(\rho'/\Lambda)^4$. Knowing this factor and α, one can obtain the value of the lightest neutrino mass, which together with the data on Δm^2_{21} and $\Delta m^2_{31(32)}$ allows one to obtain the values of the other two light neutrino masses. Knowing the latter one can find also the two ratios of the heavy Majorana neutrino masses.

In the case of NO neutrino mass spectrum ($\phi = 0$), there are two values of α that satisfy Eq. (4.13) for $r = 0.032$: $\alpha \cong 1.20$ (solution A), and $\alpha \cong 0.79$ (solution B). In the case of solution A, as it is not difficult to show, the phases

$$\phi_2 = 0, \qquad \phi_3 = 0, \qquad \text{solution A (NO)}, \tag{4.14}$$

and the three neutrino masses have the values

[3]We are following in this part the similar analysis performed in Ref. [36].

$$m_1 \cong 4.44 \times 10^{-3}\ \mathrm{eV}, \quad m_2 \cong 9.77 \times 10^{-3}\ \mathrm{eV}, \quad m_3 \cong 4.89 \times 10^{-2}\ \mathrm{eV}, \quad \text{solution A (NO)}. \tag{4.15}$$

Evidently, the spectrum is mildly hierarchical. The ratios of the heavy Majorana neutrino masses read $M_1/M_3 \cong 11.0$ and $M_2/M_3 \cong 5.0$. Thus, we have $M_3 < M_2 < M_1$.

For solution B we find

$$\phi_2 = 0, \qquad \phi_3 = \pi, \qquad \text{solution B (NO)}, \tag{4.16}$$

while for the values of the three neutrino masses we get

$$m_1 \cong 5.89 \times 10^{-3}\ \mathrm{eV}, \quad m_2 \cong 1.05 \times 10^{-2}\ \mathrm{eV}, \quad m_3 \cong 4.90 \times 10^{-2}\ \mathrm{eV}, \quad \text{solution B (NO)}. \tag{4.17}$$

The heavy Majorana neutrino mass ratios are given by $M_1/M_3 \cong 8.33$ and $M_2/M_3 \cong 4.67$. Therefore also in this case we have $M_3 < M_2 < M_1$.

For the IO spectrum ($\phi = \pi$), we find only one value of α which satisfies Eq. (4.13) with $r = 0.032$: $\alpha \cong 2.014$. The phases ϕ_2 and ϕ_3 take the values: $\phi_2 = \pi$, $\phi_3 = 0$. The light neutrino masses read

$$m_1 \cong 5.17 \times 10^{-2}\ \mathrm{eV}, \quad m_2 \cong 5.24 \times 10^{-2}\ \mathrm{eV}, \quad m_3 \cong 1.74 \times 10^{-2}\ \mathrm{eV}\ (\mathrm{IO}), \tag{4.18}$$

i.e., the light neutrino mass spectrum is not hierarchical exhibiting only partial hierarchy. For the heavy Majorana neutrino mass ratios we obtain: $M_1/M_2 \cong 1.014$ and $M_3/M_2 \cong 3.01$. Thus, in this case N_1 and N_2 are quasidegenerate in mass: $M_1 \cong M_2 < M_3$.

In the Figs. 2 and 3 we present the dependence of the neutrino masses with respect to r for normal and inverted ordering, respectively.

B. The mixing angles and the Dirac and Majorana *CP* violation phase

The PMNS neutrino mixing matrix received contributions from the diagonalization of the neutrino Majorana mass matrix M_ν and of the charged lepton mass matrix $M_e = v_d Y_e$: $U_{\mathrm{PMNS}} = U^\dagger_{eL} U_\nu$, where U_ν is given in Eq. (4.9) with $\tilde{Q} = \mathrm{Diag}(1, e^{\mathrm{i}\phi_2/2}, e^{\mathrm{i}\phi_3/2})$ and the values of the phases ϕ_2 and ϕ_3 in the cases of NO and IO spectra were specified in the preceding subsection. The matrix of charged lepton Yukawa couplings Y_e, Eq. (3.5), and thus M_e, has a block-diagonal form. The unitary matrix U_{eL} diagonalizes the Hermitian matrix $M^\dagger_e M_e$: $M^\dagger_e M_e = U_{eL}(M^d_e)^2 U^\dagger_{eL}$, where $M^d_e = \mathrm{diag}(m_e, m_\mu, m_\tau)$, m_l being the mass of the charged lepton l. As a consequence of the block-diagonal form of M_e, the matrix U_{eL} can be parametrized in terms of one mixing angle (θ^e_{12}) and one phase (φ): $U_{eL} = \Phi R_{12}(\theta^e_{12})$, where $\Phi = \mathrm{diag}(1, \mathrm{e}^{\mathrm{i}\varphi}, 1)$ and

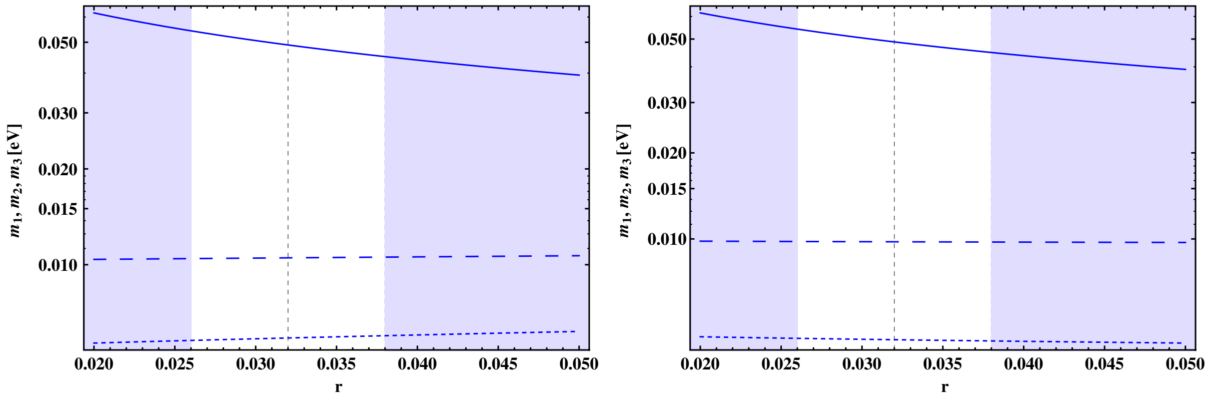

FIG. 2 (color online). The values of the three light neutrino masses corresponding to the solutions A (left panel) and B (right panel) in the case of the NO spectrum, versus r. The dotted, dashed, and solid lines correspond to the three light neutrino masses m_1, m_2, m_3. The gray region is excluded by present oscillation data. The vertical dashed line corresponds to the best fit value for $r = 0.032$. See text for further details.

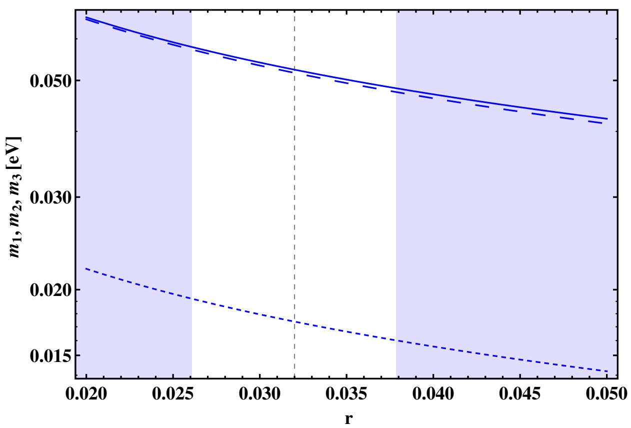

FIG. 3 (color online). The values of the three light neutrino masses in the case of the solution corresponding to the IO spectrum, versus r. The dotted, dashed, and solid lines correspond to the three light neutrino masses m_3, m_1, m_2. The gray region is excluded by present oscillation data. The vertical dashed line corresponds to the best fit value for $r = 0.032$.

$$R_{12}(\theta_{12}^e) = \begin{pmatrix} \cos\theta_{12}^e & \sin\theta_{12}^e & 0 \\ -\sin\theta_{12}^e & \cos\theta_{12}^e & 0 \\ 0 & 0 & 1 \end{pmatrix}. \tag{4.19}$$

Because of the $SU(5)$ symmetry of the model, Y_d and Y_e (and therefore the corresponding down quark and charged lepton mass matrices) are expressed in terms of the same parameters. As a consequence, the angle θ_{12}^e in the model considered is related to the Cabibbo angle $\theta^c \cong 0.226$. Using, for example, the approximate formulas from Ref. [16], we find that

$$\theta_{12}^e \cong \left|\frac{b_d'}{b_d}\right| \theta^c \cong 0.9\theta^c, \tag{4.20}$$

where we have used the values of b_d' and b_d from Table IV.

Comparing next the expressions on the two sides of the equation $M_e^\dagger M_e = U_{eL}(M_e^d)^2 U_{eL}^\dagger$ we get, in particular,

$$\mathrm{e}^{-\mathrm{i}(\varphi+\frac{\pi}{2})}(m_\mu^2 - m_e^2)\cos\theta_{12}^e \sin\theta_{12}^e = v_d^2\left(\frac{3}{2}b_d a_d - 36 c_d b_d'\right). \tag{4.21}$$

Using the fit results in Table IV one can check that the right-hand side of the last equation is real and positive. Comparing the phases of the two expressions one concludes that

$$\varphi = \frac{3}{2}\pi. \tag{4.22}$$

In the approximation we are using the PMNS matrix is given by

$$\tilde{U}_{\mathrm{PMNS}} = \begin{pmatrix} \sqrt{2/3}c_{12}^e + \sqrt{1/6}s_{12}^e e^{-\mathrm{i}\varphi} & \sqrt{1/3}c_{12}^e - \sqrt{1/3}s_{12}^e e^{-\mathrm{i}\varphi} & \sqrt{1/2}s_{12}^e e^{-\mathrm{i}\varphi} \\ \sqrt{2/3}s_{12}^e - \sqrt{1/6}c_{12}^e \mathrm{e}^{-\mathrm{i}\varphi} & \sqrt{1/3}s_{12}^e + \sqrt{1/3}c_{12}^e \mathrm{e}^{-\mathrm{i}\varphi} & -\sqrt{1/2}c_{12}^e \mathrm{e}^{-\mathrm{i}\varphi} \\ -\sqrt{1/6} & \sqrt{1/3} & \sqrt{1/2} \end{pmatrix} \tilde{Q}, \tag{4.23}$$

where $c_{12}^e = \cos\theta_{12}^e$, $s_{12}^e = \sin\theta_{12}^e$, and $\tilde{Q}$ is the diagonal phase matrix defined in Eq. (4.9). It follows from the above expression for the PMNS matrix that the angle θ_{13} is given approximately by

$$\sin^2\theta_{13} \cong \frac{1}{2}C^2\sin^2\theta^c \cong \frac{\sin^2\theta^c}{2.5} \cong 0.02, \qquad C \cong 0.9, \tag{4.24}$$

where we took into account the relation in Eq. (4.20) and the value of $C \equiv |b_d'/b_d|$.

As was shown in, e.g., Ref. [16], the phase φ and the Dirac phase δ in Eqs. (1.1) and (1.2) are related (at leading order) as follows:

$$\delta = \varphi + \pi. \tag{4.25}$$

Thus, for the Dirac phase we get from (4.22):

$$\delta = \frac{\pi}{2}. \tag{4.26}$$

Numerically, for $\varphi = 3\pi/2$ and $s_{12}^e = 0.203$ [see Eq. (4.20)], the PMNS matrix, Eq. (4.23), reads

$$U_{\rm PMNS} \cong \begin{pmatrix} 0.804e^{i5.81^\circ} & 0.577e^{-i11.50^\circ} & 0.144e^{-i270.000^\circ} \\ 0.433e^{-i67.85^\circ} & 0.577e^{i78.50^\circ} & -0.692e^{-i270.000^\circ} \\ -0.408 & 0.577 & 0.707 \end{pmatrix}\tilde{Q}. \tag{4.27}$$

Thus, comparing the absolute values of the elements U_{e1}, U_{e2}, $U_{\mu3}$, and $U_{\tau3}$ of the PMNS matrix in the standard parametrization, Eq. (1.1), and in Eq. (4.27), we have $c_{12}c_{13} = 0.804$, $s_{12}c_{13} = 0.577$, $s_{23}c_{13} = 0.692$, and $c_{23}c_{13} = 0.707$. Using the predicted value of θ_{13}, Eq. (4.24), these relations allow us to obtain the values of θ_{12} and θ_{23}. We note that the tribimaximal mixing value of the solar neutrino mixing angle θ_{12}, which corresponds to $\sin^2\theta_{12} = 1/3$, is corrected by a quantity which, as it follows from the general form of such corrections [14–16], is determined by the angle θ_{13} and the Dirac phase δ:

$$\sin^2\theta_{12} \cong \frac{1}{3} + \frac{2\sqrt{2}}{3}\sin\theta_{13}\cos\delta, \tag{4.28}$$

where δ is the Dirac phase in the standard parametrization of the PMNS matrix. As we have seen, to leading order $\delta = \pi/2$. The Majorana phases β_1, β_2 (or α_{21} and α_{31}) are determined, as it follows from Eqs. (1.1) and (4.23) [or (4.27)], by the diagonal matrix $\tilde{Q}$ and take CP conserving values. Note, however, that the parametrization of the PMNS matrix in Eq. (4.27) differs from the standard one: it corresponds to one of the several possible parametrizations of the PMNS matrix [15]. Thus, in order to get the values of the Dirac and Majorana phases δ and β_1, β_2 (or α_{21}, α_{31}) of the standard parametrization of the PMNS matrix, one has to bring the expressions (4.27) in a form that corresponds to the "standard" one in Eq. (1.1). This can be done by using the freedom of multiplying the rows of the PMNS matrix with arbitrary phases and by shifting some of the common phases of the columns to a diagonal phase matrix P. The results for the numerical matrix in Eq. (4.27) is

$$U_{\rm PMNS} \cong \begin{pmatrix} 0.804 & 0.577 & 0.144e^{-i84.25^\circ} \\ -0.433e^{i10.59^\circ} & 0.577e^{-i5.75^\circ} & 0.692 \\ 0.408e^{-i11.56^\circ} & -0.577e^{i5.75^\circ} & 0.707 \end{pmatrix}P\tilde{Q}, \tag{4.29}$$

where $\tilde{Q} = (1, e^{i\phi_2/2}, e^{i\phi_3/2}) = e^{i\phi_3/2}{\rm Diag}(e^{-i\phi_3/2}, e^{-i(\phi_3-\phi_2)/2}, 1)$ and the new phase matrix $P = {\rm Diag}(e^{i11.50^\circ}, e^{-i5.81^\circ}, -1)$. Now comparing Eq. (4.29) with Eq. (1.1) we can obtain the values of the Dirac and the two Majorana phases of the standard parametrization of the PMNS matrix, predicted by the model. For the Dirac phase we find $\delta \cong 84.3^\circ$. Note that the Majorana phases $\beta_1/2$ and $\beta_2/2$ (or $\alpha_{21}/2$ and $\alpha_{31}/2$) in the standard parametrization are not CP conserving [23]; due to the matrix P they get CP violating corrections to the CP conserving values 0 and $\pi/2$ or $3\pi/2$.

As we have seen, the value of the Dirac phase δ predicted by the model is close to $\pi/2$. This implies that the magnitude of the CP violation effects in neutrino oscillations is also predicted to be relatively large. Indeed, the rephasing invariant associated with the Dirac phase [37], $J_{CP} = {\rm Im}(U_{e1}^* U_{\mu1} U_{e3} U_{\mu3}^*)$, which determines the magnitude of CP violation effects in neutrino oscillations [38], has the following value:

$$J_{CP} = 0.0324. \tag{4.30}$$

The values we have obtained for both $\sin\theta_{13}$ and δ are in very good agreement with the numerical results in Table VI derived using the REAP package [34].

TABLE VI. Numerical results for the neutrino sector. The experimental results are taken from Ref. [6] apart from the value for θ_{13}, which is the Daya Bay result [7].

Quantity	Experiment (2σ ranges)	Model
$\sin^2\theta_{12}$	0.275–0.342	0.340
$\sin^2\theta_{23}$	0.36–0.60	0.490
$\sin^2\theta_{13}$	0.015–0.032	0.020
δ	...	84.3°

It is possible to derive simple analytic expressions that explain the numerical results obtained above and quoted in Table VI. Indeed, up to corrections of order $(\theta^e_{12})^2$ we have

$$\theta_{12} = \arcsin\frac{1}{\sqrt{3}} + \frac{\sqrt{2}}{8}(\theta^e_{12})^2, \tag{4.31}$$

$$\theta_{13} = \frac{1}{\sqrt{2}}\theta^e_{12}, \tag{4.32}$$

$$\theta_{23} = \frac{\pi}{4} - \frac{1}{4}(\theta^e_{12})^2, \tag{4.33}$$

$$\delta = \frac{\pi}{2} - \frac{1}{2}\theta^e_{12}, \tag{4.34}$$

$$\beta_1 = 2\pi - 2\theta^e_{12} + \phi_3, \tag{4.35}$$

$$\beta_2 = 2\pi + \theta^e_{12} + \phi_3 - \phi_2, \tag{4.36}$$

where $\theta^e_{12} \cong 0.888\theta^c$. Note that the expression for δ is correct up to $\mathcal{O}(\theta^e_{12})$ only because it appears always with θ_{13}, which is of order θ^e_{12} itself. Numerically, these approximations give for $\theta^e_{12} = 0.2$:

$$\sin^2\theta_{12} = 0.340, \tag{4.37}$$

$$\sin^2\theta_{13} = 0.020, \tag{4.38}$$

$$\sin^2\theta_{23} = 0.490, \tag{4.39}$$

$$\delta = 84.3°, \tag{4.40}$$

$$\beta_1 = 337.1° + \phi_3, \tag{4.41}$$

$$\beta_2 = 11.5° + \phi_3 - \phi_2. \tag{4.42}$$

As we see, the results obtained using the approximate analytic expressions are in very good agreement with those derived in the numerical analysis.

Note that all these relations were derived neglecting RGE corrections. Indeed they are under control. For the inverted ordering the RGE corrections can be expected to be largest, because there m_1 and m_2 are almost equal [39]. We have found numerically with the REAP package [34] that the biggest deviation is in δ, which goes down to 81.2°. The Majorana phases run less than 1° and also the mixing angles stay well within their two sigma ranges.

C. Predictions for other observables in the neutrino sector

We derive in this section the predictions for the sum of the neutrino masses and the effective Majorana mass $|\langle m\rangle|$ in neutrinoless double beta decay (see, e.g., Ref. [40]) using the standard parametrization of the PMNS mixing matrix as in (1.2) and the results on the neutrino masses, mixing angles, and CP violation phases obtained in the preceding subsections of this section.

In the case of solution A for the NO neutrino mass spectrum we get for the sum of the neutrino masses

$$\sum_{k=1}^{3} m_k = 6.31\times 10^{-2}\ \text{eV}, \qquad \text{solution A (NO)}. \tag{4.43}$$

In this case we have $\phi_2 = \phi_3 = 0$ (see Sec. IV A) and for the effective Majorana mass we obtain using Eqs. (4.15) and (4.29)

$$\begin{aligned}|\langle m\rangle| &= \left|\sum_{k=1}^{3}(U_{\text{PMNS}})^2_{ek}m_k\right| \\ &= 4.90\times 10^{-3}\ \text{eV}, \qquad \text{solution A (NO)}.\end{aligned} \tag{4.44}$$

The same quantities for solution B of the NO spectrum have the values:

$$\sum_{k=1}^{3} m_k = 6.54\times 10^{-2}\ \text{eV}, \qquad \text{solution B (NO)}, \tag{4.45}$$

and

$$|\langle m\rangle| = 7.95\times 10^{-3}\ \text{eV}, \qquad \text{solution B (NO)}, \tag{4.46}$$

where we have used the fact that for solution B we have $\phi_2 = 0$ and $\phi_3 = \pi$. As a consequence, in particular of the values of $\phi_{2,3}$, the three terms in the expression for $|\langle m\rangle|$ essentially add.

Finally, in the case of the IO spectrum we obtain

$$\sum_{k=1}^{3} m_k = 12.1\times 10^{-2}\ \text{eV (IO)}, \tag{4.47}$$

and

$$|\langle m\rangle| = 2.17\times 10^{-2}\ \text{eV (IO)}. \tag{4.48}$$

We recall that for the IO spectrum we have $\phi_2 = \pi$ and $\phi_3 = 0$, and there is a partial compensation in $|\langle m\rangle|$ between the dominant contributions due to the terms $\propto m_1$ and $\propto m_2$.

V. SUMMARY AND CONCLUSIONS

We have presented here the first $SU(5)\times T'$ unified model of flavor, which predicts the reactor neutrino mixing angle θ_{13} to be in the range determined by

Daya Bay [7] and RENO [8] experiments, and all other mixing angles are predicted to have values within the experimental uncertainties. It implements a type I seesaw mechanism and from the breaking of the discrete family symmetry T', we obtain tribimaximal mixing in the neutrino sector. The relatively large value of θ_{13} is then generated entirely by corrections coming from the charged lepton sector. This is a generic effect in GUTs where Yukawa couplings are related to each other. Here we have used recently proposed $SU(5)$ GUT relations [24] between the down-type quark Yukawa matrix and the charged lepton Yukawa matrix to get the relatively large prediction for the reactor mixing angle θ_{13} along the lines proposed in Refs. [16,29].

The corrections to the solar and the atmospheric neutrino mixing angle are under control due to the structure of the charged lepton Yukawa matrix and the pattern of the complex CP violation phases. The model exhibits a special kind of CP violation, the so-called ''geometrical'' CP violation. All parameters and vevs are real and all nontrivial phases are coming from the complex Clebsch-Gordan coefficients of T' and are integer multiples of $\pi/4$. We have given the renormalizable superpotential that generates effectively the Yukawa matrices after integrating out heavy messenger fields and plugging in the family symmetry breaking flavon vevs, which was missing so far in the literature for $SU(5) \times T'$ models. The flavon vevs point in special directions in flavor space and are all real. These results come out as solutions to the flavon alignment superpotential we have presented in the Appendix C.

We have shown, in particular, that the phase pattern in the Yukawa matrices actually gives a good fit of the quark and charged lepton masses and the CKM parameters at low energies. This fit fixes the charged lepton Yukawa matrix completely and since we find tribimaximal mixing in the neutrino sector itself, we can make predictions for the neutrino masses and all PMNS parameters. The angle θ_{13} is predicted to have a value corresponding to $\sin^2\theta_{13} \cong 0.8\sin^2\theta^c/2 = 0.02$. For the Dirac phase δ we obtain in the standard parametrization of the PMNS matrix $\delta = 84.3°$. Our model also predicts $\sin^2\theta_{12} = 0.340$ and $\sin^2\theta_{23} = 0.490$. There are three different possible solutions for the neutrino masses, two with normal ordering (solutions A and B) and one with inverted ordering. All three cases can be tested in experiments determining the absolute neutrino mass scale (or the sum of the three neutrino masses), in experiments that can measure the solar and atmospheric neutrino mixing angles with a high precision, in experiments searching for CP violation in neutrino oscillations, and in neutrinoless double beta decay experiments. For the sum of three neutrino masses we get [with relatively small uncertainties; see Figs. 2 and 3]: $\sum_{k=1}^{3} m_k = 6.31 \times 10^{-2}$ eV (NO, A); 6.54×10^{-2} eV (NO, B), and 12.1×10^{-2} eV (IO). The $(\beta\beta)_{0\nu}$-decay effective Majorana mass for the three solutions is also unambiguously predicted: $|\langle m \rangle| = 4.90 \times 10^{-3}$ eV (NO, A); 7.95×10^{-3} eV (NO, B); 2.17×10^{-2} eV (IO). The three solutions differ only in the values of the three neutrino masses and of the Majorana phases, so that we make one single prediction for the rephasing invariant that determines the magnitude of CP violation effects in neutrino oscillations: $J_{CP} = 0.0324$. This value of J_{CP} is relatively large and can be tested in the experiments on CP violation in neutrino oscillations.

In conclusion, with the recent measurement of the last unknown neutrino mixing angle, neutrino physics has entered a new era. All angles are determined with a rather good precision, constraining flavor models severely. Since θ_{13} turned out to be relatively large, the observation of CP violation in the lepton sector might be feasible with data from the running and upcoming neutrino oscillation experiments. Explaining the data on leptonic CP violation would pose another challenge for flavor models. The model we proposed here is from this point of view rather comprehensive combining many ideas that have been proposed elsewhere but have been combined here consistently for the first time. Because of the GUT structure we can fit the quark masses and mixing parameters and the charged lepton masses, and using the latter we make definite predictions for the neutrino mass spectrum, the leptonic mixing angles, and the leptonic CP violating phases. Our model is therefore testable in a variety of experiments. We are looking forward to the outcome of these tests.

ACKNOWLEDGMENTS

We would like to thank Christoph Luhn and Ferruccio Feruglio for useful discussions. This work was supported in part by the INFN program on ''Astroparticle Physics,'' by the Italian MIUR program on ''Neutrinos, Dark Matter and Dark Energy in the Era of LHC'' (A. M. and S. T. P.), and by the World Premier International Research Center Initiative (WPI Initiative), MEXT, Japan (S. T. P.). Furthermore the authors acknowledge partial support from the European Union under FP7 ITN INVISIBLES (Marie Curie Actions, PITN-GA-2011-289442).

APPENDIX A: T': THE RULES OF THE GAME

T' is the double-covering group of the tetrahedral symmetry T that is isomorphic to A_4, the group of the even permutations of four objects. T' contains three inequivalent one-dimensional representations, called $\mathbf{1}$, $\mathbf{1}'$, and $\mathbf{1}''$, one three-dimensional, $\mathbf{3}$, and three two-dimensional representations, $\mathbf{2}$, $\mathbf{2}'$, and $\mathbf{2}''$. Two of these representations are real, $\mathbf{1}$ and $\mathbf{3}$, one is pseudoreal $\mathbf{2}$, and the other four are complex. We list in Table VII the relevant tensor products of T'. For more details on T', see, e.g., Ref. [17] and references therein.

TABLE VII. The Clebsch-Gordan coefficients for the tensor products of T'.

$$a\otimes\Gamma^p = a\Gamma^p,\ a\otimes a'(a'') = a'(a''),\ a'\otimes a'(a'') = a''(a),\ a'(a'')\otimes a'' = a(a')$$

$$\begin{pmatrix}x_1\\x_2\end{pmatrix}_{\mathbf{2}}\otimes a'(a'') = \begin{pmatrix}x_1a'(a'')\\x_2a'(a'')\end{pmatrix}_{\mathbf{2}'(\mathbf{2}'')},\ \begin{pmatrix}y_1\\y_2\end{pmatrix}_{\mathbf{2}'}\otimes a'(a'') = \begin{pmatrix}y_1a'(a'')\\y_2a'(a'')\end{pmatrix}_{\mathbf{2}''(\mathbf{2})},\ \begin{pmatrix}z_1\\z_2\end{pmatrix}_{\mathbf{2}''}\otimes a'(a'') = \begin{pmatrix}z_1a'(a'')\\z_2a'(a'')\end{pmatrix}_{\mathbf{2}(\mathbf{2}')}$$

$$\begin{pmatrix}x_1\\x_2\end{pmatrix}_{\mathbf{2}(\mathbf{2}')}\otimes\begin{pmatrix}x'_1\\x'_2\end{pmatrix}_{\mathbf{2}(\mathbf{2}'')} = \left(\frac{x_1x'_2-x_2x'_1}{\sqrt{2}}\right)_{\mathbf{1}}\oplus\begin{pmatrix}\frac{(1-\mathrm{i})}{2}(x_1x'_2+x_2x'_1)\\ \mathrm{i}x_1x'_1\\ x_2x'_2\end{pmatrix}_{\mathbf{3}}$$

$$\begin{pmatrix}y_1\\y_2\end{pmatrix}_{\mathbf{2}'(\mathbf{2})}\otimes\begin{pmatrix}y'_1\\y'_2\end{pmatrix}_{\mathbf{2}'(\mathbf{2}'')} = \left(\frac{y_1y'_2-y_2y'_1}{\sqrt{2}}\right)_{\mathbf{1}''}\oplus\begin{pmatrix}\mathrm{i}y_1y'_1\\ y_2y'_2\\ \frac{(1-\mathrm{i})}{2}(y_1y'_2+y_2y'_1)\end{pmatrix}_{\mathbf{3}}$$

$$\begin{pmatrix}z_1\\z_2\end{pmatrix}_{\mathbf{2}''(\mathbf{2})}\otimes\begin{pmatrix}z'_1\\z'_2\end{pmatrix}_{\mathbf{2}''(\mathbf{2}')} = \left(\frac{z_1z'_2-z_2z'_1}{\sqrt{2}}\right)_{\mathbf{1}'}\oplus\begin{pmatrix}z_2z'_2\\ \frac{(1-\mathrm{i})}{2}(z_1z'_2+z_2z'_1)\\ \mathrm{i}z_1z'_1\end{pmatrix}_{\mathbf{3}}$$

$$(a')_{\mathbf{1}'}\otimes\begin{pmatrix}u_1\\u_2\\u_3\end{pmatrix}_{\mathbf{3}} = \begin{pmatrix}u_3a'\\u_1a'\\u_2a'\end{pmatrix}_{\mathbf{3}},\ (a'')_{\mathbf{1}''}\otimes\begin{pmatrix}u_1\\u_2\\u_3\end{pmatrix}_{\mathbf{3}} = \begin{pmatrix}u_2a''\\u_3a''\\u_1a''\end{pmatrix}_{\mathbf{3}}$$

$$\begin{pmatrix}x_1\\x_2\end{pmatrix}_{\mathbf{2}}\otimes\begin{pmatrix}u_1\\u_2\\u_3\end{pmatrix}_{\mathbf{3}} = \frac{1}{\sqrt{3}}\left[\begin{pmatrix}(1+\mathrm{i})x_2u_2+x_1u_1\\(1-\mathrm{i})x_1u_3-x_2u_1\end{pmatrix}_{\mathbf{2}}\oplus\begin{pmatrix}(1+\mathrm{i})x_2u_3+x_1u_2\\(1-\mathrm{i})x_1u_1-x_2u_2\end{pmatrix}_{\mathbf{2}'}\oplus\begin{pmatrix}(1+\mathrm{i})x_2u_1+x_1u_3\\(1-\mathrm{i})x_1u_2-x_2u_3\end{pmatrix}_{\mathbf{2}''}\right]$$

$$\begin{pmatrix}y_1\\y_2\end{pmatrix}_{\mathbf{2}'}\otimes\begin{pmatrix}u_1\\u_2\\u_3\end{pmatrix}_{\mathbf{3}} = \frac{1}{\sqrt{3}}\left[\begin{pmatrix}(1+\mathrm{i})y_2u_1+y_1u_3\\(1-\mathrm{i})y_1u_2-y_2u_3\end{pmatrix}_{\mathbf{2}}\oplus\begin{pmatrix}(1+\mathrm{i})y_2u_2+y_1u_1\\(1-\mathrm{i})y_1u_3-y_2u_1\end{pmatrix}_{\mathbf{2}'}\oplus\begin{pmatrix}(1+\mathrm{i})y_2u_3+y_1u_2\\(1-\mathrm{i})y_1u_1-y_2u_2\end{pmatrix}_{\mathbf{2}''}\right]$$

$$\begin{pmatrix}z_1\\z_2\end{pmatrix}_{\mathbf{2}''}\otimes\begin{pmatrix}u_1\\u_2\\u_3\end{pmatrix}_{\mathbf{3}} = \frac{1}{\sqrt{3}}\left[\begin{pmatrix}(1+\mathrm{i})z_2u_3+z_1u_2\\(1-\mathrm{i})z_1u_1-z_2u_2\end{pmatrix}_{\mathbf{2}}\oplus\begin{pmatrix}(1+\mathrm{i})z_2u_1+z_1u_3\\(1-\mathrm{i})z_1u_2-z_2u_3\end{pmatrix}_{\mathbf{2}'}\oplus\begin{pmatrix}(1+\mathrm{i})z_2u_2+z_1u_1\\(1-\mathrm{i})z_1u_3-z_2u_1\end{pmatrix}_{\mathbf{2}''}\right]$$

$$\begin{pmatrix}u_1\\u_2\\u_3\end{pmatrix}_{\mathbf{3}}\otimes\begin{pmatrix}u'_1\\u'_2\\u'_3\end{pmatrix}_{\mathbf{3}} = \frac{1}{\sqrt{3}}[(u_1u'_1+u_2u'_3+u_3u'_2)_{\mathbf{1}}\oplus(u_1u'_2+u_2u'_1+u_3u'_3)_{\mathbf{1}'}\oplus(u_1u'_3+u_2u'_2+u_3u'_1)_{\mathbf{1}''}]$$

$$\oplus\frac{1}{\sqrt{6}}\begin{pmatrix}2u_1u'_1-u_2u'_3-u_3u'_2\\2u_3u'_3-u_1u'_2-u_2u'_1\\2u_2u'_2-u_1u'_3-u_3u'_1\end{pmatrix}_{\mathbf{3}}\oplus\frac{1}{\sqrt{2}}\begin{pmatrix}u_2u'_3-u_3u'_2\\u_1u'_2-u_2u'_1\\u_3u'_1-u_1u'_3\end{pmatrix}_{\mathbf{3}}$$

APPENDIX B: MESSENGER SECTOR

In our model we consider nonrenormalizable operators. In general the contraction of the $SU(5)$ and T' indices may not be unique, which is nevertheless essential for our model. Our predictions are based on the fact that only a certain contraction is allowed as we have, for example, indicated in Eq. (3.2) for the T' indices. For the connection between the so-called UV completion and predictivity of a model, see also Ref. [41]. Hence we have to specify the so-called messenger fields that generate only the desired contractions in the operators after being integrated out in a specific order.

The full list of messenger fields of our model is given in Table VIII. Every messenger pair in every line receives a mass term in the superpotential, like, for example, $M_{\Sigma_1^a}\Sigma_1^a\bar{\Sigma}_1^a$. For the sake of brevity we do not write down all of the mass terms, but it is important to note that there are no mass terms between messengers in different lines allowed. We assume all the messenger masses to be above the scale of T' and $SU(5)$ breaking, which are closely related in our model as we will see in the next section. Many messengers carry $SU(5)$ quantum numbers so that above the messenger scale, which we denote by Λ, the gauge coupling becomes quickly nonperturbative, so that we are not predictive above this scale.

Having given these general remarks, we now turn to the superpotential that describes the couplings of the various fields to the messengers. We start with the messengers coupling to the matter, Higgs fields, and flavon fields. The supergraphs showing these couplings are given in Figs. 4–6. From these diagrams one can read off all the relevant contractions and couplings. Nevertheless, we give now the renormalizable superpotential containing the messenger fields.

Apart from the messenger mass terms (which we do not write down explicitly) there are no terms with one or two fields involving matter, Higgs fields, and flavon fields. For the down-type quark diagrams we find (here and in this whole section we do not write down the couplings)

TABLE VIII. Messenger fields used in our model. After integrating out these fields we end up with the desired effective operators. For the sake of brevity we do not list all of the mass terms in the text. The messenger pair in every line has a mass term and there are no cross terms allowed.

Messenger fields	$SU(5)$	T'	$U(1)_R$	Z_{12}^u	Z_8^d	Z_8^ν	Z_8	Z_6	Z_6^l	Z_4
Σ_1^a, $\bar\Sigma_1^a$	$\mathbf{1}$, $\mathbf{1}$	$\mathbf{1}$, $\mathbf{1}$	0, 2	4, 8	0, 0	0, 0	0, 0	2, 4	2, 4	0, 0
Σ_1^b, $\bar\Sigma_1^b$	$\mathbf{1}$, $\mathbf{1}$	$\mathbf{1}$, $\mathbf{1}$	0, 2	4, 8	0, 0	0, 0	0, 0	0, 0	0, 0	0, 0
$\Sigma_{1'}^a$, $\bar\Sigma_{1''}^a$	$\mathbf{1}$, $\mathbf{1}$	$\mathbf{1}'$, $\mathbf{1}''$	0, 2	6, 6	4, 4	4, 4	4, 4	0, 0	0, 0	2, 2
$\Sigma_{1'}^b$, $\bar\Sigma_{1''}^b$	$\mathbf{1}$, $\mathbf{1}$	$\mathbf{1}'$, $\mathbf{1}''$	0, 2	8, 4	4, 4	4, 4	4, 4	4, 2	4, 2	0, 0
$\Sigma_{1'}^c$, $\bar\Sigma_{1''}^c$	$\mathbf{1}$, $\mathbf{1}$	$\mathbf{1}'$, $\mathbf{1}''$	0, 2	8, 4	0, 0	0, 0	0, 0	2, 4	2, 4	0, 0
$\Sigma_{1''}^a$, $\bar\Sigma_{1'}^a$	$\mathbf{1}$, $\mathbf{1}$	$\mathbf{1}''$, $\mathbf{1}'$	0, 2	6, 6	4, 4	0, 0	4, 4	1, 5	1, 5	0, 0
$\Sigma_{1''}^b$, $\bar\Sigma_{1'}^b$	$\mathbf{1}$, $\mathbf{1}$	$\mathbf{1}''$, $\mathbf{1}'$	0, 2	0, 0	6, 2	2, 6	6, 2	3, 3	3, 3	0, 0
$\Sigma_{1''}^c$, $\bar\Sigma_{1'}^c$	$\mathbf{24}$, $\mathbf{24}$	$\mathbf{1}''$, $\mathbf{1}'$	0, 2	3, 9	2, 6	0, 0	6, 2	0, 0	3, 3	1, 3
$\Sigma_{2''}^a$, $\bar\Sigma_{2'}^a$	$\mathbf{1}$, $\mathbf{1}$	$\mathbf{2}''$, $\mathbf{2}'$	0, 2	9, 3	5, 3	7, 1	1, 7	3, 3	3, 3	3, 1
$\Sigma_{2''}^b$, $\bar\Sigma_{2'}^b$	$\mathbf{1}$, $\mathbf{1}$	$\mathbf{2}''$, $\mathbf{2}'$	0, 2	9, 3	4, 4	5, 3	3, 5	4, 2	1, 5	2, 2
Σ_3^a, $\bar\Sigma_3^a$	$\mathbf{1}$, $\mathbf{1}$	$\mathbf{3}$, $\mathbf{3}$	0, 2	6, 6	4, 4	0, 0	4, 4	1, 5	1, 5	0, 0
Σ_3^b, $\bar\Sigma_3^b$	$\mathbf{1}$, $\mathbf{1}$	$\mathbf{3}$, $\mathbf{3}$	0, 2	0, 0	6, 2	2, 6	6, 2	3, 3	3, 3	0, 0
Σ_3^c, $\bar\Sigma_3^c$	$\mathbf{1}$, $\mathbf{1}$	$\mathbf{3}$, $\mathbf{3}$	0, 2	0, 0	0, 0	4, 4	0, 0	3, 3	3, 3	2, 2
Σ_3^d, $\bar\Sigma_3^d$	$\mathbf{1}$, $\mathbf{1}$	$\mathbf{3}$, $\mathbf{3}$	0, 2	0, 0	0, 0	0, 0	4, 4	0, 0	3, 3	2, 2
$\Xi_{1'}^a$, $\bar\Xi_{1''}^a$	$\mathbf{5}$, $\bar{\mathbf{5}}$	$\mathbf{1}'$, $\mathbf{1}''$	1, 1	5, 7	0, 0	4, 4	0, 0	5, 1	5, 1	2, 2
$\Xi_{2'}^a$, $\bar\Xi_{2''}^a$	$\mathbf{5}$, $\bar{\mathbf{5}}$	$\mathbf{2}'$, $\mathbf{2}''$	1, 1	2, 10	7, 1	5, 3	3, 5	2, 4	5, 1	3, 1
$\Xi_{2''}^a$, $\bar\Xi_{2'}^a$	$\mathbf{5}$, $\bar{\mathbf{5}}$	$\mathbf{2}''$, $\mathbf{2}'$	1, 1	8, 4	5, 3	7, 1	1, 7	2, 4	5, 1	1, 3
Ω_1^a, $\bar\Omega_1^a$	$\mathbf{5}$, $\bar{\mathbf{5}}$	$\mathbf{1}$, $\mathbf{1}$	0, 2	2, 10	0, 0	2, 10	4, 4	5, 1	5, 1	0,0
$\Omega_{1'}^a$, $\bar\Omega_{1''}^a$	$\mathbf{5}$, $\bar{\mathbf{5}}$	$\mathbf{1}'$, $\mathbf{1}''$	2, 0	8, 4	0, 0	8, 4	0, 0	4, 2	4, 2	2, 2
$\Omega_{1'}^b$, $\bar\Omega_{1''}^b$	$\mathbf{5}$, $\bar{\mathbf{5}}$	$\mathbf{1}'$, $\mathbf{1}''$	2, 0	9, 3	1, 7	9, 3	2, 6	4, 2	1, 5	2, 2
$\Omega_{2''}^a$, $\bar\Omega_{2'}^a$	$\mathbf{5}$, $\bar{\mathbf{5}}$	$\mathbf{2}''$, $\mathbf{2}'$	2, 0	9, 3	2, 6	9, 3	7, 1	1, 5	4, 2	2, 2
Ω_3^a, $\bar\Omega_3^a$	$\mathbf{5}$, $\bar{\mathbf{5}}$	$\mathbf{1}$, $\mathbf{1}$	0, 2	0, 0	3, 5	0, 0	4, 4	4, 2	4, 2	1, 3
$\Upsilon_{1''}^a$, $\bar\Upsilon_{1'}^a$	$\mathbf{10}$, $\bar{\mathbf{10}}$	$\mathbf{1}''$, $\mathbf{1}'$	1, 1	2, 10	1, 7	5, 3	2, 6	3, 3	3, 3	2, 2
$\Upsilon_{1''}^b$, $\bar\Upsilon_{1'}^b$	$\mathbf{10}$, $\bar{\mathbf{10}}$	$\mathbf{1}''$, $\mathbf{1}'$	1, 1	2, 10	0, 0	3, 5	4, 4	5, 1	2, 4	3, 1
Υ_2^a, $\bar\Upsilon_2^a$	$\mathbf{10}$, $\bar{\mathbf{10}}$	$\mathbf{2}$, $\mathbf{2}$	1, 1	11, 1	0, 0	2, 6	1, 7	4, 2	1, 5	3, 1
Υ_2^b, $\bar\Upsilon_2^b$	$\mathbf{10}$, $\bar{\mathbf{10}}$	$\mathbf{2}$, $\mathbf{2}$	1, 1	5, 7	2, 6	0, 0	7, 1	0, 0	0, 0	3, 1
Υ_2^c, $\bar\Upsilon_2^c$	$\mathbf{10}$, $\bar{\mathbf{10}}$	$\mathbf{2}$, $\mathbf{2}$	1, 1	5, 7	6, 2	4, 4	3, 5	0, 0	0, 0	3, 1
$\Upsilon_{2'}^a$, $\bar\Upsilon_{2''}^a$	$\mathbf{10}$, $\bar{\mathbf{10}}$	$\mathbf{2}'$, $\mathbf{2}''$	1, 1	11, 1	0, 0	2, 6	1, 7	4, 2	1, 5	3, 1
$\Upsilon_{2'}^b$, $\bar\Upsilon_{2''}^b$	$\mathbf{10}$, $\bar{\mathbf{10}}$	$\mathbf{2}'$, $\mathbf{2}''$	1, 1	5, 7	0, 0	4, 4	7, 1	4, 2	1, 5	3, 1
$\Upsilon_{2'}^c$, $\bar\Upsilon_{2''}^c$	$\mathbf{10}$, $\bar{\mathbf{10}}$	$\mathbf{2}'$, $\mathbf{2}''$	1, 1	5, 7	2, 6	0, 0	7, 1	0, 0	0, 0	3, 1
$\Upsilon_{2'}^d$, $\bar\Upsilon_{2''}^d$	$\mathbf{10}$, $\bar{\mathbf{10}}$	$\mathbf{2}'$, $\mathbf{2}''$	1, 1	11, 1	0, 0	2, 6	5, 3	2, 4	5, 1	3, 1
$\Upsilon_{2''}^a$, $\bar\Upsilon_{2'}^a$	$\mathbf{10}$, $\bar{\mathbf{10}}$	$\mathbf{2}''$, $\mathbf{2}'$	1, 1	5, 7	4, 4	0, 0	7, 1	3, 3	0, 0	1, 3
$\Upsilon_{2''}^b$, $\bar\Upsilon_{2'}^b$	$\mathbf{10}$, $\bar{\mathbf{10}}$	$\mathbf{2}''$, $\mathbf{2}'$	1, 1	11, 1	0, 0	2, 6	1, 7	4, 2	1, 5	3, 1
$\Upsilon_{2''}^c$, $\bar\Upsilon_{2'}^c$	$\mathbf{10}$, $\bar{\mathbf{10}}$	$\mathbf{2}''$, $\mathbf{2}'$	1, 1	2, 10	2, 6	6, 2	7, 1	0, 0	3, 3	0, 0
$\Upsilon_{2''}^d$, $\bar\Upsilon_{2'}^d$	$\mathbf{10}$, $\bar{\mathbf{10}}$	$\mathbf{2}''$, $\mathbf{2}'$	1, 1	11, 1	0, 0	2, 6	5, 3	2, 4	5, 1	3, 1
$\Upsilon_{2''}^e$, $\bar\Upsilon_{2'}^e$	$\mathbf{10}$, $\bar{\mathbf{10}}$	$\mathbf{2}''$, $\mathbf{2}'$	1, 1	11, 1	0, 0	6, 2	5, 3	0, 0	0, 0	1, 3
Υ_3^a, $\bar\Upsilon_3^a$	$\mathbf{10}$, $\bar{\mathbf{10}}$	$\mathbf{3}$, $\mathbf{3}$	1, 1	2, 10	0, 0	7, 1	4, 4	4, 2	1, 5	1, 3
Υ_3^b, $\bar\Upsilon_3^b$	$\mathbf{10}$, $\bar{\mathbf{10}}$	$\mathbf{3}$, $\mathbf{3}$	1, 1	8, 4	0, 0	5, 3	2, 6	2, 4	5, 1	1, 3
Υ_3^c, $\bar\Upsilon_3^c$	$\mathbf{10}$, $\bar{\mathbf{10}}$	$\mathbf{3}$, $\mathbf{3}$	1, 1	8, 4	2, 6	5, 3	6, 2	5, 1	5, 1	3, 1
Υ_3^d, $\bar\Upsilon_3^d$	$\mathbf{10}$, $\bar{\mathbf{10}}$	$\mathbf{3}$, $\mathbf{3}$	1, 1	2, 10	5, 3	5, 3	6, 2	3, 3	0, 0	0, 0
$\Gamma_{2''}^a$, $\bar\Gamma_{2'}^a$	$\mathbf{24}$, $\mathbf{24}$	$\mathbf{2}''$, $\mathbf{2}'$	2, 0	9, 3	3, 5	5, 3	7, 1	3, 3	0, 0	1, 3

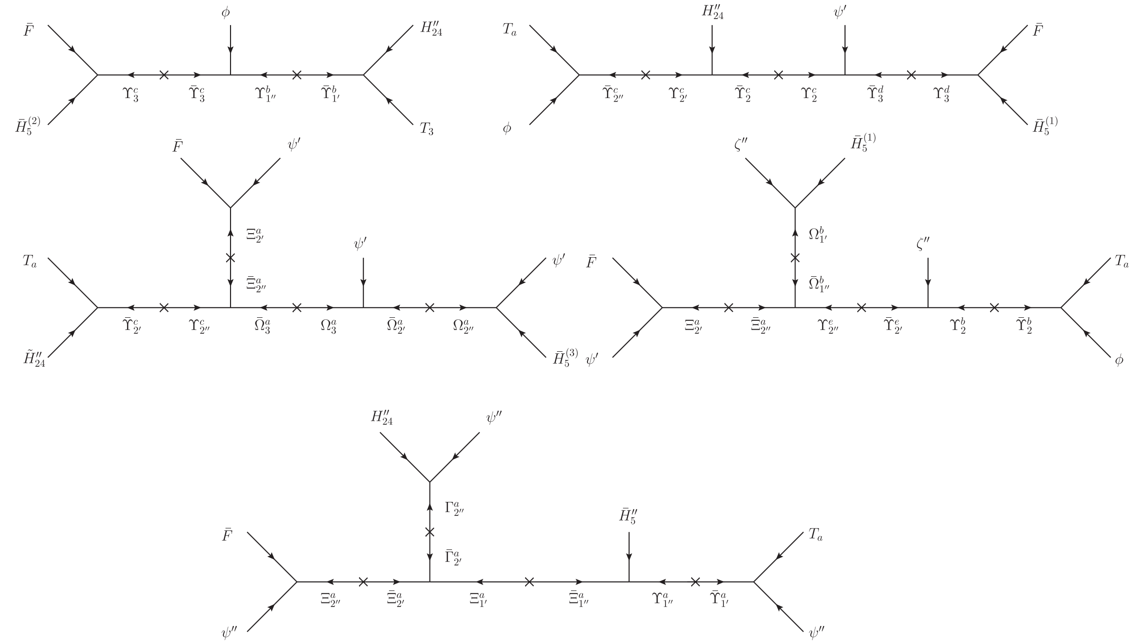

FIG. 4. The supergraphs before integrating out the messengers for the down-type quark and charged lepton sector.

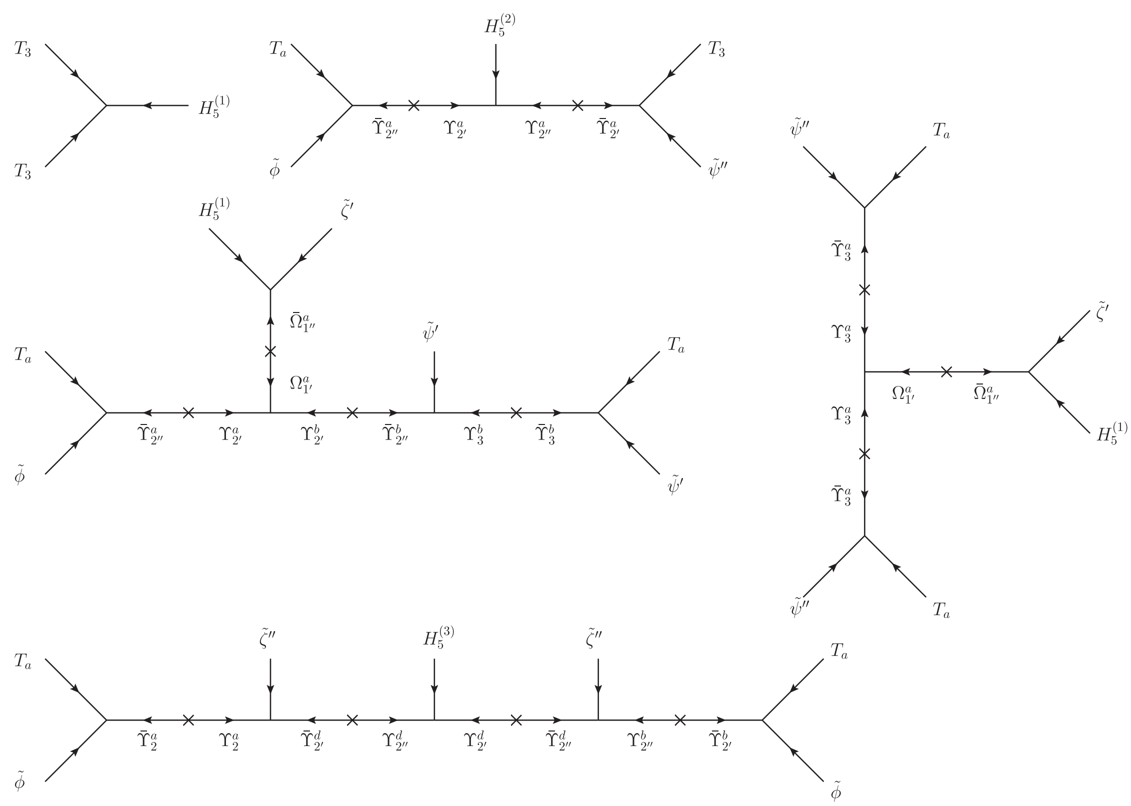

FIG. 5. The supergraphs before integrating out the messengers for the up-type quark sector.

$$\mathcal{W}_d^{\rm ren} = \bar{F}\bar{H}_5^{(2)}\Upsilon_3^c + \phi\bar{\Upsilon}_3^c\Upsilon_{1''}^b + H_{24}''T_3\bar{\Upsilon}_{1'}^b \tag{B1}$$

$$+ T_a\phi\bar{\Upsilon}_{2''}^c + H_{24}''\bar{\Upsilon}_2^c\Upsilon_{2'}^c + \psi'\Upsilon_2^c\bar{\Upsilon}_3^d + \bar{F}\bar{H}_5^{(1)}\Upsilon_3^d \tag{B2}$$

$$+ T_a\tilde{H}_{24}''\bar{\Upsilon}_{2'}^c + \bar{H}_5^{(3)}\psi'\Omega_{2''}^a + \bar{\Omega}_{2'}^a\psi'\Omega_3^a + \bar{\Omega}_3^a\Upsilon_{2''}^c\bar{\Xi}_{2''}^a \tag{B3}$$

$$+ \bar{F}\psi'\Xi_{2'}^a + \bar{\Xi}_{2''}^a\Upsilon_{2''}^e\bar{\Omega}_{1''}^b + \zeta''\bar{H}_5^{(1)}\Omega_{1'}^b + \zeta''\bar{\Upsilon}_{2'}^e\Upsilon_2^b + T_a\phi\bar{\Upsilon}_2^b \tag{B4}$$

$$+ \bar{F}\psi''\Xi_{2''}^a + \bar{\Xi}_{2'}^a\Xi_{1'}^a\bar{\Gamma}_{2'}^a + H_{24}''\psi''\Gamma_{2''}^a + \bar{H}_5''\bar{\Xi}_{1''}^a\Upsilon_{1''}^a + \bar{\Upsilon}_{1'}^aT_a\psi'', \tag{B5}$$

for the up-type quarks

$$\mathcal{W}_u^{\rm ren} = H_5^{(1)}T_3^2 + T_a\tilde{\phi}\bar{\Upsilon}_{2''}^a + H_5^{(2)}\Upsilon_{2'}^a\Upsilon_{2''}^a + T_3\tilde{\psi}''\bar{\Upsilon}_{2'}^a \tag{B6}$$

$$+ T_a\tilde{\psi}''\bar{\Upsilon}_3^a + \tilde{\zeta}'H_5^{(1)}\bar{\Omega}_{1''}^a + \Omega_{1'}^a\Upsilon_3^a\Upsilon_3^a \tag{B7}$$

$$+ T_a\tilde{\phi}\bar{\Upsilon}_{2''}^a + \Upsilon_{2'}^a\Omega_{1'}^a\Upsilon_{2'}^b + H_5^{(1)}\tilde{\zeta}'\bar{\Omega}_{1''}^a + \tilde{\psi}'\bar{\Upsilon}_{2''}^b\Upsilon_3^b + \bar{\Upsilon}_3^bT_a\tilde{\psi}' \tag{B8}$$

$$+ T_a\tilde{\phi}\bar{\Upsilon}_2^a + \Upsilon_2^a\tilde{\zeta}''\bar{\Upsilon}_{2'}^d + H_5^{(3)}\Upsilon_{2''}^d\Upsilon_{2'}^d + \tilde{\zeta}''\bar{\Upsilon}_{2''}^d\Upsilon_{2''}^b + T_a\tilde{\phi}\bar{\Upsilon}_{2'}^b, \tag{B9}$$

and for the neutrino sector

$$\mathcal{W}_\nu^{\rm ren} = N^2\xi + N^2\rho + N^2\tilde{\rho} + \bar{F}N\Omega_1^a + H_5^{(2)}\rho\bar{\Omega}_1^a + H_5^{(2)}\tilde{\rho}\bar{\Omega}_1^a. \tag{B10}$$

There are five additional operators that generate dimension eight or more operators in the matter sector, which we neglect. For completeness we give them as well:

$$\mathcal{W}_{d\geq 8}^{\rm ren,matter} = \zeta'\Upsilon_2^c\bar{\Upsilon}_{2''}^c + \bar{\Upsilon}_2^c\Upsilon_3^d\psi'' + \psi''\Omega_{2''}^a\bar{\Omega}_3^a + \bar{\Gamma}_{2'}^a\bar{\Upsilon}_{2''}^c\Upsilon_3^d + \bar{\Gamma}_{2'}^a\bar{\Upsilon}_2^b\Upsilon_3^d. \tag{B11}$$

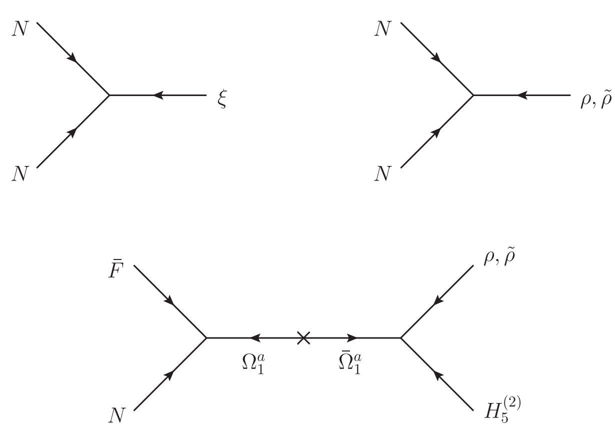

FIG. 6. The supergraphs before integrating out the messengers for the neutrino sector.

We turn now to the messengers, which give the nonrenormalizable terms in the flavon alignment superpotential that we denote collectively with Σ. In this sector all of the supergraphs have the structure as given in Fig. 7. (The role of the auxiliary ϵ fields is described in the next section and their quantum numbers are given in Table X.) For the sake of brevity we do not give all the diagrams for the flavon sector, but all diagrams can easily be derived from the renormalizable flavon superpotential. We give here only the terms where a messenger is involved. The terms that have no messenger involved will be discussed in the next section, when we discuss the superpotential responsible for the flavon alignment. The superpotential involving the Σ fields reads

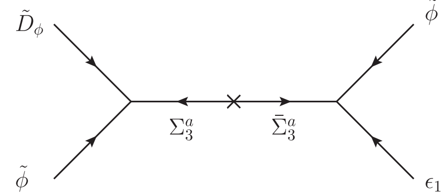

FIG. 7. One typical diagram for the messengers in the flavon sector. We consider only effective operators up to dimension four. For the sake of brevity we only show one diagram. The others are quite similar with the driving field on one side and the auxiliary ϵ fields on the other side.

$$\mathcal{W}_{\Sigma}^{\text{ren}} = D_{\xi}\xi\Sigma_3^c + D_{\xi}\rho\Sigma_3^c + D_{\xi}\tilde{\rho}\Sigma_3^c + \bar{\Sigma}_3^c\xi\epsilon_9 + \tilde{D}_{\phi}\tilde{\phi}\Sigma_3^a + \bar{\Sigma}_3^a\tilde{\phi}\epsilon_1 \tag{B12}$$

$$+ \tilde{D}_{\phi}\tilde{\phi}\Sigma_{1''}^a + \bar{\Sigma}_{1'}^a\tilde{\zeta}''\epsilon_2 + D_{\phi}\phi\Sigma_3^b + \bar{\Sigma}_3^b\phi\epsilon_4 + D_{\phi}\phi\Sigma_{1''}^b + \bar{\Sigma}_{1'}^b\zeta''\epsilon_5 \tag{B13}$$

$$+ D_{\psi}\psi''\Sigma_{2''}^a + \bar{\Sigma}_{2'}^a\psi''\epsilon_6 + D_{\psi}\phi\Sigma_{1'}^a + S_{\zeta}''\epsilon_7\Sigma_{1'}^a + \bar{\Sigma}_{1''}^a\zeta'\epsilon_7 + S_1\psi'\Sigma_{2''}^b + \bar{\Sigma}_{2'}^b\tilde{\psi}''\epsilon_8 \tag{B14}$$

$$+ S_2'\zeta'\Sigma_{1'}^b + \bar{\Sigma}_{1''}^b\zeta'\epsilon_{12} + S_2'\tilde{\zeta}'\Sigma_{1'}^c + \bar{\Sigma}_{1''}^c\tilde{\zeta}'\epsilon_{13} + S_{\epsilon_{12}}\epsilon_{12}\Sigma_1^a + \bar{\Sigma}_1^a\epsilon_{12}^2 \tag{B15}$$

$$+ S_{\epsilon_{13}}\epsilon_{13}\Sigma_1^b + \bar{\Sigma}_1^b\epsilon_{13}^2 + \tilde{S}_{24}''\tilde{H}_{24}''\Sigma_{1''}^c + \bar{\Sigma}_{1'}^c\epsilon_{10}\tilde{H}_{24}'' + \tilde{S}_{24}''\xi\Sigma_3^d + \bar{\Sigma}_3^d\epsilon_{11}\xi. \tag{B16}$$

Apart from these there are as well operators that give dimension five operators in the flavon alignment superpotential after integrating out the messenger fields, which we will neglect. These operators are

$$\mathcal{W}_{d\geq 5}^{\text{ren,flavon}} = S_{\zeta}''\Sigma_1^a\Sigma_{1'}^b + S_{\tilde{\zeta}}''\Sigma_1^b\Sigma_{1'}^c + S_{\tilde{\zeta}}''\Sigma_{1''}^a\Sigma_{1''}^a + S_{\zeta}''\Sigma_{1''}^b\Sigma_{1''}^b + S_{\tilde{\zeta}}''\Sigma_3^a\Sigma_3^a + S_{\zeta}''\Sigma_3^b\Sigma_3^b \tag{B17}$$

$$+ S_{24}''\Sigma_3^c\Sigma_3^c + S_{24}''\Sigma_3^d\Sigma_3^d + (S_{\epsilon_i} + S_{\xi} + S_{\rho})\Sigma_3^c\Sigma_3^c + (S_{\epsilon_i} + S_{\xi} + S_{\rho})\Sigma_3^d\Sigma_3^d. \tag{B18}$$

Now we have discussed the messenger sector. After integrating out the messengers from the renormalizable superpotential we end up with the effective operators that give us the desired flavon vev alignments and structures of the Yukawa matrices.

APPENDIX C: FLAVON VACUUM ALIGNMENT

In this appendix we present the solution for our flavon vacuum alignment. In the present model, all of the discussed results crucially depend on the vev structure and on the fact that all flavon vevs are real.

In the flavon potential two new kinds of fields are introduced. First we have to add driving fields that are gauge singlets but transform in a nontrivial way under the family and shaping symmetries and have a $U(1)_R$ charge of two. Minimizing the F term equations of these fields will give us the correct alignment (including phases) as one possible solution. Second we introduce auxiliary fields ϵ_i, $i = 1, \ldots, 13$, which are singlets under $SU(5)$ and T', but they transform in a nontrivial way under the additional shaping symmetries. They appear only in the flavon superpotential. Indeed, these fields are introduced to compensate the charges of different operators, so that they are related to each other in the F term equations. Note that we have to include for our alignment nonrenormalizable operators, where we restrict ourselves to operators with mass dimension not higher than four in the superpotential. The driving fields are listed in Table IX and the auxiliary fields are listed in Table X.

Before going into the more complicated details of the flavon vacuum alignment, we briefly discuss the "alignment" of the auxiliary flavons, which is simply the question of how to give them a real vev. For this purpose we used the simple idea advocated in Ref. [42], which we can directly illustrate at the alignment for the ϵ fields itself. The superpotential for their alignment reads

$$\mathcal{W}_{\epsilon} = S_{\epsilon_i}(\epsilon_i^2 - M_{\epsilon_i}^2) + S_{\epsilon_j}\left(\frac{1}{\Lambda}\epsilon_j^3 - M_{\epsilon_j}^2\right), \tag{C1}$$

where $i = 1, \ldots, 11$ and $j = 12, 13$. Note that for the sake of readability we do not include any couplings. The driving fields S_{ϵ_i} and S_{ϵ_j} are total singlets so that terms like $S_{\epsilon}M_{\epsilon}^2$

TABLE IX. List of the driving fields from the superpotential that give the desired vacuum alignment. All driving fields are $SU(5)$ gauge singlets and charged under $U(1)_R$ with charge $+2$.

	$\tilde{D}_{\phi}$	$\tilde{S}_{\psi}$	$\tilde{S}_{\zeta}''$	$\tilde{S}_{\zeta}$	D_{ϕ}	D_{ψ}	S_{ζ}''	D_{ξ}	S_{ξ}	S_{ρ}	S_{24}''	$\tilde{S}_{24}''$	S_1	S_2'	S_{ϵ_i}
T'	**3**	**1**	$\mathbf{1}''$	**1**	**3**	**3**	$\mathbf{1}''$	**3**	**1**	**1**	$\mathbf{1}''$	$\mathbf{1}''$	**1**	$\mathbf{1}'$	**1**
Z_{12}^u	6	0	0	0	6	0	0	6	0	0	0	6	6	4	0
Z_8^d	4	0	0	0	0	2	4	4	0	0	0	4	5	0	0
Z_8^{ν}	4	0	0	0	4	2	4	4	0	0	0	0	2	0	0
Z_8	0	4	0	4	0	2	4	4	0	0	0	0	2	0	0
Z_6	1	0	4	0	3	0	0	3	0	0	0	0	5	2	0
Z_6'	1	0	4	0	0	3	0	3	0	0	0	3	5	2	0
Z_4	0	0	0	0	0	2	0	2	0	0	0	2	1	0	0

TABLE X. List of the auxiliary flavon fields that do not couple to the matter sector. The ϵ_i fields are all $SU(5) \times T'$ singlets and carry no $U(1)_R$ charge.

	ϵ_1	ϵ_2	ϵ_3	ϵ_4	ϵ_5	ϵ_6	ϵ_7	ϵ_8	ϵ_9	ϵ_{10}	ϵ_{11}	ϵ_{12}	ϵ_{13}
Z_{12}^u	6	6	0	6	6	6	6	6	6	0	6	8	8
Z_8^d	4	4	0	4	0	4	0	4	4	0	0	0	4
Z_8^ν	4	0	0	0	4	0	0	4	4	0	0	0	0
Z_8	0	0	4	4	0	4	0	4	4	4	0	0	0
Z_6	3	3	0	3	3	0	0	0	3	0	0	4	0
Z_6'	3	3	0	3	3	0	0	0	3	0	0	4	0
Z_4	0	0	0	0	2	0	2	0	2	0	2	0	0

are allowed. The F term equations for the driving fields give, e.g.,

$$F_{S_{\epsilon_1}} = \epsilon_1^2 - M_{\epsilon_1}^2 = 0. \tag{C2}$$

And since we assume that our fundamental theory is CP conserving, the mass M_{ϵ_1} is real (like the coupling parameters, which are not shown) and, hence, the vev of ϵ_1 is real and nonvanishing. For ϵ_{12} and ϵ_{13} this has to be slightly modified. For those we find three possible solutions, two of them complex and only one real. But we assume that the real solution is picked up, which could be preferred by higher order corrections, supergravity corrections, or some low-energy soft terms in the scalar potential. To discuss these corrections in detail is beyond the scope of the current paper.

Note also that all of the S_{ϵ_i} driving fields have the same quantum numbers and hence can mix with each other. In other words, each of these driving fields could couple to each ϵ field. We have chosen here the basis in which the superpotential has the above structure, which makes the alignment clear (see also the appendix of Ref. [42]).

The same method can be applied to the real triplet and singlet flavons of our model, after we have fixed their alignment by some different kind of operators. But for the complex doublets ($\mathbf{2}'$, $\mathbf{2}''$) and singlets ($\mathbf{1}'$, $\mathbf{1}''$) we have to use other relations, because the representation squared cannot form a total singlet.

Before we come to these complex representations we discuss the alignment for the flavons appearing in the neutrino sector (ξ, ρ, $\tilde{\rho}$) where this complication is absent.[4] The superpotential for these flavons reads

$$\mathcal{W}_{\xi,\rho,\tilde{\rho}} = \frac{D_\xi}{\Lambda}(\xi^2\epsilon_9 + \xi\rho\epsilon_9 + \xi\tilde{\rho}\epsilon_9) + S_\xi(\xi^2 - M_\xi^2) + S_\rho(\rho^2 + \tilde{\rho}^2 - M_\rho^2). \tag{C3}$$

The first thing to note here is that we used the auxiliary flavon ϵ_9 in the first set of operators involving the triplet driving field D_ξ. Since ϵ_9 appears in all three operators, it drops out in the F term conditions, but nevertheless it is real and hence would just modify the value of the vev without introducing any phase. The F term conditions are

$$\frac{\partial \mathcal{W}_{\xi,\rho,\tilde{\rho}}}{\partial D_{\xi_1}} = 2\xi_1^2 - 2\xi_2\xi_3 + \xi_1(\rho + \tilde{\rho}) = 0, \tag{C4}$$

$$\frac{\partial \mathcal{W}_{\xi,\rho,\tilde{\rho}}}{\partial D_{\xi_2}} = 2\xi_2^2 - 2\xi_1\xi_3 + \xi_3(\rho + \tilde{\rho}) = 0, \tag{C5}$$

$$\frac{\partial \mathcal{W}_{\xi,\rho,\tilde{\rho}}}{\partial D_{\xi_3}} = 2\xi_3^2 - 2\xi_2\xi_1 + \xi_2(\rho + \tilde{\rho}) = 0, \tag{C6}$$

$$\frac{\partial \mathcal{W}_{\xi,\rho,\tilde{\rho}}}{\partial S_\xi} = \xi_1^2 + 2\xi_2\xi_3 - M_\xi^2 = 0, \tag{C7}$$

$$\frac{\partial \mathcal{W}_{\xi,\rho,\tilde{\rho}}}{\partial S_\rho} = \rho^2 + \tilde{\rho}^2 - M_\rho^2 = 0. \tag{C8}$$

Besides the trivial solution $\xi_i = 0$, $i = 1, 2, 3$, we find for the first three of these equations by cyclic permutations in ξ_i the desired solution for which $\xi_i = \xi_0 \neq 0$ if $\rho_0 = -\tilde{\rho}_0$. The fact that the vevs are nonvanishing and real can then be read off from the last two equations for which we used the method from Ref. [42] discussed above.

Now we come to the most complicated part of the flavon alignment sector, the flavons present in the quark and charged lepton sectors. Although we have two different sets of flavons, one for the up-quark sector on the one hand and one for the down-type quark and charged lepton sector on the other hand, we cannot separate their alignments completely. In fact, we found that the alignments themselves are independent from each other, but the simplest solution that we found to make all vevs real involves cross couplings between the two sectors. The flavon superpotential reads

[4] The alignment for the triplets follows the discussion in the seminal paper [43].

$$\mathcal{W}_f = \frac{\tilde{D}_\phi}{\Lambda}(\tilde{\phi}\,\tilde{\phi}\,\epsilon_1 + \tilde{\phi}\tilde{\zeta}''\epsilon_2) + \tilde{S}''_\zeta(\tilde{\zeta}''\tilde{\zeta}'' + \tilde{\phi}\,\tilde{\phi} - M_{\tilde{\zeta}'}\tilde{\zeta}') + \tilde{S}_\zeta(\tilde{\zeta}'\tilde{\zeta}'' - M_{\tilde{\zeta}}\epsilon_3) \tag{C9}$$

$$+ \tilde{S}_\psi(\tilde{\psi}'\tilde{\psi}'' - \tilde{\zeta}'\tilde{\zeta}'') + \frac{D_\phi}{\Lambda}(\phi\phi\epsilon_4 + \phi\zeta''\epsilon_5) + \frac{D_\psi}{\Lambda}((\psi'')^2\epsilon_6 + \phi\zeta'\epsilon_7) \tag{C10}$$

$$+ S_\psi(\psi'\psi'' - M_\psi^2) + S''_\zeta\left(\zeta''\zeta'' + \phi\phi - M_{\zeta'}\zeta' + \frac{\epsilon_7^2}{\Lambda}\zeta'\right) \tag{C11}$$

$$+S_1\left(\psi'\tilde{\psi}''\frac{\epsilon_8}{\Lambda} - M_{S_1}^2\right) + S'_2((\zeta')^2\epsilon_{12} - (\tilde{\zeta}')^2\epsilon_{13}), \tag{C12}$$

where in the last equations the cross couplings between the two sectors are written. We do not want to discuss here the whole alignment extensively; instead we will only discuss the phases of the vevs of the complex fields in a bit more detail. Nevertheless, we quote all the F term conditions, in which it is then quite easy to plug in the flavon vevs from Eqs. (2.1), (2.2), and (2.3) and see that they form a viable solution. The F term conditions read for the up sector

$$\frac{\partial\mathcal{W}_f}{\partial\tilde{D}_{\phi_1}} = \epsilon_1(2\tilde{\phi}_1^2 - 2\tilde{\phi}_2\tilde{\phi}_3) + \epsilon_2\tilde{\phi}_2\tilde{\zeta}'' = 0, \tag{C13}$$

$$\frac{\partial\mathcal{W}_f}{\partial\tilde{D}_{\phi_2}} = \epsilon_1(2\tilde{\phi}_2^2 - 2\tilde{\phi}_1\tilde{\phi}_3) + \epsilon_2\tilde{\phi}_1\tilde{\zeta}'' = 0, \tag{C14}$$

$$\frac{\partial\mathcal{W}_f}{\partial\tilde{D}_{\phi_3}} = \epsilon_1(2\tilde{\phi}_3^2 - 2\tilde{\phi}_1\tilde{\phi}_2) + \epsilon_2\tilde{\phi}_3\tilde{\zeta}'' = 0, \tag{C15}$$

$$\frac{\partial\mathcal{W}_f}{\partial\tilde{S}''_\zeta} = (\tilde{\zeta}'')^2 - M_{\tilde{\zeta}'}\tilde{\zeta}' + \tilde{\phi}_3^2 + 2\tilde{\phi}_1\tilde{\phi}_2 = 0, \tag{C16}$$

$$\frac{\partial\mathcal{W}_f}{\partial\tilde{S}_\zeta} = \tilde{\zeta}'\tilde{\zeta}'' - M_{\tilde{\zeta}}\epsilon_3 = 0, \tag{C17}$$

$$\frac{\partial\mathcal{W}_f}{\partial\tilde{S}_\psi} = \tilde{\psi}'_1\tilde{\psi}''_2 - \tilde{\psi}'_2\tilde{\psi}''_1 - \tilde{\zeta}'\tilde{\zeta}'' = 0, \tag{C18}$$

for the down sector

$$\frac{\partial\mathcal{W}_f}{\partial D_{\phi_1}} = \epsilon_4(2\phi_1^2 - 2\phi_2\phi_3) + \epsilon_5\phi_2\zeta'' = 0, \tag{C19}$$

$$\frac{\partial\mathcal{W}_f}{\partial D_{\phi_2}} = \epsilon_4(2\phi_2^2 - 2\phi_1\phi_3) + \epsilon_5\phi_1\zeta'' = 0, \tag{C20}$$

$$\frac{\partial\mathcal{W}_f}{\partial D_{\phi_3}} = \epsilon_4(2\phi_3^2 - 2\phi_1\phi_2) + \epsilon_5\phi_3\zeta'' = 0, \tag{C21}$$

$$\frac{\partial\mathcal{W}_f}{\partial D_{\psi_1}} = \epsilon_6((\psi''_2)^2 + \epsilon_7\phi_3\zeta' = 0, \tag{C22}$$

$$\frac{\partial\mathcal{W}_f}{\partial D_{\psi_2}} = \mathrm{i}\epsilon_6((\psi''_1)^2 + \epsilon_7\phi_2\zeta' = 0, \tag{C23}$$

$$\frac{\partial\mathcal{W}_f}{\partial D_{\psi_3}} = (1-\mathrm{i})\epsilon_6\psi''_1\psi''_2 + \epsilon_7\phi_1\zeta' = 0, \tag{C24}$$

$$\frac{\partial\mathcal{W}_f}{\partial S_\psi} = \psi'_1\psi''_2 - \psi'_2\psi''_1 - M_\psi^2 = 0, \tag{C25}$$

$$\frac{\partial\mathcal{W}_f}{\partial S''_\zeta} = (\zeta'')^2 - \left(M_{\zeta'} + \frac{\epsilon_7^2}{\Lambda}\right)\zeta' = 0, \tag{C26}$$

and for the cross couplings between the two sectors

$$\frac{\partial\mathcal{W}_f}{\partial S_1} = (\psi'_1\tilde{\psi}''_2 - \psi'_2\tilde{\psi}''_1)\frac{\epsilon_8}{\Lambda} - M_{S_1}^2 = 0, \tag{C27}$$

$$\frac{\partial\mathcal{W}_f}{\partial S'_2} = (\zeta')^2\epsilon_{12} - (\tilde{\zeta}')^2\epsilon_{13} = 0. \tag{C28}$$

So how do we make the vevs of the complex representations real? Exemplary we discuss the complex singlets $\tilde{\zeta}''$, $\tilde{\zeta}'$, ζ'', and ζ'. From Eqs. (C16) and (C17) we find a polynomial in $\tilde{\zeta}''$

$$(\tilde{\zeta}'')^3 + \tilde{\zeta}''(\tilde{\phi}_3^2 + 2\tilde{\phi}_1\tilde{\phi}_2) - M_{\tilde{\zeta}'}M_{\tilde{\zeta}}\epsilon_3 = 0, \tag{C29}$$

which has a real solution (at least for a certain choice of parameters and plugging in the real vev of $\tilde{\phi}$) which we pick here. Then we know that $(\tilde{\zeta}'')^3$ is real, while $\tilde{\zeta}'$ has the opposite phase of $\tilde{\zeta}''$ so it is real as well. From Eq. (C28) we then find ζ' to be real and from Eq. (C26) we obtain ζ'' to be real and all the singlet vevs are real. For the doublets a similar mechanism applies.

The last alignment we want to discuss here is, strictly speaking, not an alignment. But since we have used adjoints of $SU(5)$ in our operators to get the desired Yukawa coupling relations between the charged leptons and the down-type quarks, we add here a mechanism that generates the vev of these adjoints and also shows explicitly that they are real. For the fields H_{24}'' and $\tilde{H}_{24}''$ we can write down the following superpotential using the two driving fields S_{24}'' and $\tilde{S}_{24}''$

$$\mathcal{W}_{24} = S_{24}''(H_{24}''H_{24}'' - \xi^2) + \frac{\tilde{S}_{24}''}{\Lambda}(\tilde{H}_{24}''\tilde{H}_{24}''\epsilon_{10} - \xi^2\epsilon_{11}). \tag{C30}$$

We see that the vev of ξ triggers a vev for the two adjoint fields and even more these two vevs are directly related to the T' symmetry breaking scale. That means that in our model the GUT scale and the scale of T' coincide (up to some order one coefficients). In principle, we can again choose here between two different vevs for the adjoints: one pointing into the SM direction and the other one pointing into the $SU(4) \times U(1)$ direction and we assume the first option to be realized. We also note here that the solution of the doublet-triplet-splitting problem and hence the construction of the whole Higgs sector is clearly beyond the scope of this paper.

[1] K. Nakamura *et al.* (Particle Data Group), J. Phys. G **37**, 075021 (2010).
[2] S. M. Bilenky, J. Hosek, and S. T. Petcov, Phys. Lett. **94B**, 495 (1980).
[3] K. Abe *et al.* (T2K Collaboration), Phys. Rev. Lett. **107**, 041801 (2011).
[4] P. Adamson *et al.* (MINOS Collaboration), Phys. Rev. Lett. **107**, 181802 (2011).
[5] Y. Abe *et al.* (Double Chooz Collaboration), Phys. Rev. Lett. **108**, 131801 (2012).
[6] G. L. Fogli, E. Lisi, A. Marrone, A. Palazzo, and A. M. Rotunno, Phys. Rev. D **84**, 053007 (2011).
[7] F. P. An *et al.* (DAYA-BAY Collaboration), Phys. Rev. Lett. **108**, 171803 (2012).
[8] J. K. Ahn *et al.* (RENO Collaboration), Phys. Rev. Lett. **108**, 191802 (2012).
[9] M. Mezzetto and T. Schwetz, J. Phys. G **37**, 103001 (2010).
[10] M. Tortola, J. W. F. Valle, and D. Vanegas, Phys. Rev. D **86**, 073012 (2012).
[11] G. Mention, M. Fechner, Th. Lasserre, Th. A. Mueller, D. Lhuillier, M. Cribier, and A. Letourneau, Phys. Rev. D **83**, 073006 (2011).
[12] P. Minkowski, Phys. Lett. **67B**, 421 (1977); M. Gell-Mann, P. Ramond, and R. Slansky, Report No. CALT-68-709, 1979; in *Supergravity* (North Holland, Amsterdam, 1979); T. Yanagida, in Proceedings of the Workshop on Unified Theory and Baryon Number of the Universe, KEK, Japan, 1979 (unpublished); S. L. Glashow, NATO Advanced Study Institutes, Ser. B. Phys., Vol. 59 (1979), p. 687; R. N. Mohapatra and G. Senjanovic, Phys. Rev. Lett. **44**, 912 (1980).
[13] P. F. Harrison, D. H. Perkins, and W. G. Scott, Phys. Lett. B **530**, 167 (2002); **535**, 163 (2002); Z. Z. Xing, Phys. Lett. B **533**, 85 (2002); X. G. He and A. Zee, Phys. Lett. B **560**, 87 (2003); see also L. Wolfenstein, Phys. Rev. D **18**, 958 (1978).
[14] P. H. Frampton, S. T. Petcov, and W. Rodejohann, Nucl. Phys. **B687**, 31 (2004); A. Romanino, Phys. Rev. D **70**, 013003 (2004).
[15] K. A. Hochmuth, S. T. Petcov, and W. Rodejohann, Phys. Lett. B **654**, 177 (2007).
[16] D. Marzocca, S. T. Petcov, A. Romanino, and M. Spinrath, J. High Energy Phys. 11 (2011) 009.
[17] F. Feruglio, C. Hagedorn, Y. Lin, and L. Merlo, Nucl. Phys. **B775**, 120 (2007); **B836**, 127(E) (2010).
[18] P. H. Frampton and T. W. Kephart, Int. J. Mod. Phys. A **10**, 4689 (1995); P. H. Frampton, T. W. Kephart, and S. Matsuzaki, Phys. Rev. D **78**, 073004 (2008); D. A. Eby, P. H. Frampton, and S. Matsuzaki, Phys. Lett. B **671**, 386 (2009); P. H. Frampton and S. Matsuzaki, Phys. Lett. B **679**, 347 (2009).
[19] G. J. Ding, Phys. Rev. D **78**, 036011 (2008).
[20] J.-Q. Chen and P.-D. Fan, J. Math. Phys. (N.Y.) **39**, 5519 (1998).
[21] M.-C. Chen and K. T. Mahanthappa, Phys. Lett. B **681**, 444 (2009).
[22] M.-C. Chen and K. T. Mahanthappa, Phys. Lett. B **652**, 34 (2007).
[23] M.-C. Chen, K. T. Mahanthappa, A. Meroni, and S. T. Petcov, arXiv:1109.0731.
[24] S. Antusch and M. Spinrath, Phys. Rev. D **79**, 095004 (2009); M. Spinrath, arXiv:1009.2511.
[25] S. Antusch, S. F. King, M. Malinsky, and M. Spinrath, Phys. Rev. D **81**, 033008 (2010).
[26] Z.-z. Xing, H. Zhang, and S. Zhou, Phys. Rev. D **77**, 113016 (2008).
[27] H. Leutwyler, Nucl. Phys. B, Proc. Suppl. **94**, 108 (2001).
[28] H. Georgi and C. Jarlskog, Phys. Lett. **86B**, 297 (1979).
[29] S. Antusch and V. Maurer, Phys. Rev. D **84**, 117301 (2011).
[30] L. J. Hall, R. Rattazzi, and U. Sarid, Phys. Rev. D **50**, 7048 (1994); M. S. Carena, M. Olechowski, S. Pokorski, and C. E. M. Wagner, Nucl. Phys. **B426**, 269 (1994); R. Hempfling, Phys. Rev. D **49**, 6168 (1994); T. Blazek, S. Raby, and S. Pokorski, Phys. Rev. D **52**, 4151 (1995).
[31] S. Antusch and M. Spinrath, Phys. Rev. D **78**, 075020 (2008).
[32] S. Profumo, Phys. Rev. D **68**, 015006 (2003); H. Baer, S. Kraml, S. Sekmen, and H. Summy, J. High Energy Phys. 03 (2008) 056; H. Baer, M. Haider, S. Kraml, S. Sekmen, and H. Summy, J. Cosmol. Astropart. Phys. 02 (2009) 002; I. Gogoladze, R. Khalid, and Q. Shafi, Phys. Rev. D **79**,

115004 (2009); I. Gogoladze, R. Khalid, S. Raza, and Q. Shafi, J. High Energy Phys. 12 (2010) 055; 06 (2011) 117.

[33] S. Antusch, L. Calibbi, V. Maurer, and M. Spinrath, Nucl. Phys. **B852**, 108 (2011).

[34] S. Antusch, J. Kersten, M. Lindner, M. Ratz, and M. A. Schmidt, J. High Energy Phys. 03 (2005) 024.

[35] J. Charles, A. Höcker, H. Lacker, S. Laplace, F. R. Le Diberder, J. Malclés, J. Ocariz, M. Pivk, and L. Roos, Eur. Phys. J. C **41**, 1 (2005); arXiv:hep-ph/0406184v3; updated results and plots: http://ckmfitter.in2p3.fr; M. Bona *et al.* (UTfit Collaboration), Phys. Rev. D **76**, 014015 (2007).

[36] C. Hagedorn, E. Molinaro, and S. T. Petcov, J. High Energy Phys. 09 (2009) 115.

[37] C. Jarlskog, Z. Phys. C **29**, 491 (1985); Phys. Rev. Lett. **55**, 1039 (1985).

[38] P. I. Krastev and S. T. Petcov, Phys. Lett. B **205**, 84 (1988).

[39] S. Antusch, J. Kersten, M. Lindner, and M. Ratz, Nucl. Phys. **B674**, 401 (2003).

[40] S. M. Bilenky and S. T. Petcov, Rev. Mod. Phys. **59**, 671 (1987); S. M. Bilenky, S. Pascoli, and S. T. Petcov, Phys. Rev. D **64**, 053010 (2001); S. Pascoli and S. T. Petcov, Phys. Rev. D **77**, 113003 (2008); W. Rodejohann, Int. J. Mod. Phys. E **20**, 1833 (2011).

[41] I. de Medeiros Varzielas and L. Merlo, J. High Energy Phys. 02 (2011) 062.

[42] S. Antusch, S. F. King, C. Luhn, and M. Spinrath, Nucl. Phys. **B850**, 477 (2011).

[43] G. Altarelli and F. Feruglio, Nucl. Phys. **B741**, 215 (2006).